The Heterogeneous-Fleet Electric Vehicle Routing Problem with Nonlinear Charging Functions

Weiquan Wang[a,*], Yossiri Adulyasak[b], Jean-François Cordeau[b], Guannan He[c,*]

[a]*Department of Information Management, University of International Business and Economics, Beijing 100029, China*
[b]*HEC Montréal and GERAD, Montréal H3T 2A7, Canada*
[c]*Department of Industrial Engineering and Management, College of Engineering, Peking University, Beijing, China*

Abstract

This paper introduces the Heterogeneous-Fleet Electric Vehicle Routing Problem with Nonlinear Charging Functions (HEVRP-NL). This problem involves routing a heterogeneous fleet of electric vehicles, utilizing multiple charging modes, and accounting for time-dependent waiting time functions at charging stations. The problem is modeled using a path-based mixed-integer linear programming formulation. To solve this problem, we present an algorithmic framework that alternates between two components. The first component is an iterated local search algorithm with a problem-specific route evaluation function, which obtains local optimal solutions and generates a pool of high-quality routes. The second component is a set-partitioning model that combines a subset of routes from the pool into a feasible solution. We design HEVRP-NL benchmark instances based on the publicly available electric fleet size and mix vehicle routing problem instances, which are used to evaluate our methods. For small-scale HEVRP-NL instances, the proposed model can be employed in a general-purpose mixed integer programming solver to achieve optimal solutions or find good upper bounds. This exact approach serves as an evaluation of our heuristic algorithm's ability to attain optimal solutions rapidly. Extensive computational results on large-scale HEVRP-NL instances illustrate the advantages of considering non-linear charging functions and show the impact of waiting time at the charging stations. Finally, we conduct experiments on 120 benchmark instances for the E-VRP-NL and 168 benchmark instances for the E-FSMFTW-PR, which are the special cases of our problem. The results indicate that our algorithm outperforms existing approaches from the literature and identifies 32 new best solutions for the E-VRP-NL and 33 new best solutions for the E-FSMFTW-PR, respectively.

Keywords: Electric Vehicle Routing Problem; Heterogeneous Fleet; Nonlinear Charging Function; Iterated Local Search; Time Dependent

*Corresponding author
Email addresses: wangweiquan@uibe.edu.cn (Weiquan Wang), yossiri.adulyasak@hec.ca (Yossiri Adulyasak), jean-francois.cordeau@hec.ca (Jean-François Cordeau), gnhe@pku.edu.cn (Guannan He)

1. Introduction

Electric Vehicle Routing Problems (E-VRPs) involve designing routes to serve a set of customers using a fleet of electric vehicles (EVs), which may require trips to charging stations (CSs) to recharge their batteries. In practice, many logistics companies employ various EV types for different delivery scenarios. In addition, cities are equipped with CSs of varying power levels (Montoya et al., 2017; Keskin & Çatay, 2018; Gnann et al., 2018), each of which is associated with a non-linear charging time (Pelletier et al., 2017). With the rapid increase in the number of EVs and relatively lengthy charging times, the level of busyness (waiting/queuing time before charging) at CSs varies considerably depending on their location and the time of day (Keskin et al., 2019). The aforementioned factors (i.e., EV type, charging time, mode, and location) can have a substantial effect on the routing decisions. Several prior studies in this field have focused on one or a few of these challenges, but none of these studies has addressed these important issues in a comprehensive fashion. To this end, we aim to tackle a more comprehensive and practical E-VRP scenario: the Heterogeneous-Fleet Electric Vehicle Routing Problem with Nonlinear Charging Functions (HEVRP-NL) by incorporating the important features of the following E-VRP variants: the Electric Fleet Size and Mix Vehicle Routing Problem with Time Windows (E-FSMFTW), the E-VRP with non-linear charging functions (E-VRP-NL), and the E-VRP with time-dependent waiting times.

Hiermann et al. (2016) introduce the E-FSMFTW, and consider a full linear charging function (EV must be fully charged at CS). In this study, larger EVs have greater load capacity and can travel longer distances, while smaller EVs have lower acquisition costs. In a subsequent study, Wang & Zhao (2023) further extend the E-FSMFTW by incorporating a partial linear recharging function, resulting in the E-FSMFTW-PR. However, as stated by Uhrig et al. (2015), there are two types of linear approximations for the real charging function: the optimistic approximation and the pessimistic approximation. The former's approximate charging rate is faster than the real charging speed, which may lead to infeasible solutions in actual scenarios; the latter's approximate charging rate is slower than the real charging speed, which may result in failure to reach the optimal solution. Due to these reasons, the use of linear charging functions is inadequate for modeling the battery charging process in real-world applications.

Montoya et al. (2017) introduce the E-VRP-NL to model a more accurate charging process. In addition to a partial charging policy, the authors propose a piecewise linear approximation of the charging process. They consider multiple charging technologies that are associated with different charging speeds, such as fast, normal, and slow. Later, Keskin et al. (2019) consider the E-VRP-NL with time-dependent waiting times at CSs. To facilitate the modeling of the waiting process, they discretize the real continuous non-linear time-dependent waiting function into several time intervals

and simulate it as a piecewise linear function. However, they only consider a single charging technology. Froger et al. (2022) extend the E-VRP-NL by considering CS capacity restrictions, leading to the E-VRP-NL-C. Despite the above studies accounting for more realistic charging functions, they all assume a fleet of homogeneous EVs.

The previous E-FSMFTW studies assume a fleet of heterogeneous EVs with the same linear charging function at any CS. In contrast, we consider that each type of EV has a unique non-linear charging function at each type of CS, which is closer to reality. Furthermore, previous work on the E-VRP-NL considered homogeneous EVs or a single EV, neglecting considerations such as heterogeneous EVs, time windows, and load capacity constraints, all of which are included in our study.

The main contributions of this paper are the following. First, we propose a general mixed-integer linear programming (MILP) model for the HEVRP-NL, which can handle both the E-VRP-NL and the E-FSMF. More specifically, the model incorporates the presence of a heterogeneous EV fleet, as well as the utilization of non-linear charging and waiting time functions into E-VRPs. Second, we propose an algorithmic framework that alternates between two components: (i) an iterated local search algorithm with a problem-specific route evaluation function, which is used to find local optimal solutions and generate a pool of high-quality routes; (ii) a set-partitioning model, which is used to combine a subset of routes from the pool into a feasible solution. Third, we conduct extensive computational experiments on HEVRP-NL benchmark instances. The results indicate that accounting for non-linear charging functions can significantly reduce logistics costs. Finally, the heuristic is compared with the state-of-the-art algorithms on 120 benchmark E-VRP-NL instances and 168 E-FSMFTW-PR instances. Our heuristic finds 32 new best solutions for the E-VRP-NL and 33 new best solutions for the E-FSMFTW-PR, respectively.

2. Literature Review

There is a vast body of literature on E-VRPs. Some studies focus on the energy consumption (Zhang et al., 2018; Pelletier et al., 2019; Basso et al., 2021; Bruglieri et al., 2023), while others focus on the battery-swapping technology (Hof et al., 2017; Jie et al., 2019; Raeesi & Zografos, 2020; Çatay & Sadati, 2023). However, the majority of papers, including this one, focus on the charging process, which is the key component in E-VRPs. In this section, we review the literature based on the type of charging functions considered.

2.1. E-VRPs with linear charging functions

First, we discuss the literature on E-VRPs with linear charging functions that focus on homogeneous EV fleets. In Schneider et al. (2014), the authors propose a mathematical model and a variable

neighborhood search algorithm with tabu search (VNS/TS) for the electric vehicle routing problem with time windows (EVRPTW) with a full linear recharging function. They aim to minimize the number of vehicles used and the total distance of routes. Felipe et al. (2014) introduce the green vehicle routing problem with multiple charging technologies and partial linear charging functions (GVRP-MTPR). Desaulniers et al. (2016) propose an exact branch-price-and-cut algorithm and investigate four different linear recharging strategies for the EVRPTW. Desaulniers et al. (2020) improve upon previous results in Desaulniers et al. (2016) by modifying the route-generation labeling algorithm and, as a consequence, they can determine additional optimal solutions. Keskin & Çatay (2016) extend the EVRPTW by using a partial linear recharging function. Schiffer & Walther (2017) focus on the electric location routing problem with time windows and partial linear recharging (ELRP-TWPR), considering location decisions for charging stations and routing of electric vehicles. In their subsequent work, Schiffer & Walther (2018) propose an adaptive large neighborhood search for the location routing problem with intra-route facilities and linear refueling policy. Cortés-Murcia et al. (2019) present the electric vehicle routing problem with time windows, partial linear recharging function, and satellite customers. Keskin et al. (2021) consider the EVRPTW with stochastic waiting times, using linear charging function.

Second, we review the literature on mixed and heterogeneous fleets. Goeke & Schneider (2015) propose the EVRPTW with a mixed fleet (EVRPTW-MF) containing electric commercial vehicles (ECVs) and conventional internal combustion commercial vehicles (ICCVs). They utilize a realistic energy consumption function that considers vehicle speed, gradients, and cargo load. Macrina et al. (2019) investigate a mixed fleet VRP with different linear recharging speeds, comprising both EVs and ICCVs. Hiermann et al. (2016) consider a variety of electric vehicles with different capacities, battery sizes, and prices and propose the E-FSMFTW, using a full linear recharging function. Hiermann et al. (2019) propose a hybrid heterogeneous electric fleet routing problem (H2E-FTW) with conventional, plug-in hybrid, and electric vehicles. Recently, Wang & Zhao (2023) extend the E-FSMFTW by incorporating a partial linear recharging function.

A notable limitation of the aforementioned literature is that the authors consider linear charging functions, which is typically not the case in practice.

2.2. E-VRPs with non-linear charging functions

Non-linear charging functions capture the fact that the battery charge level is not a linear function of the charging time (Uhrig et al., 2015). This consideration is aligned with reality and also leads to improved routing decisions in terms of feasibility and operating costs (Pelletier et al., 2017). Therefore, studies on E-VRP-NLs have gained attention in recent years. This literature often relies on either

one of the following assumptions: 1) the CSs can simultaneously handle an unlimited number of EVs, or 2) each CS is equipped with a limited number of available chargers.

First, we provide a review of the literature assuming the CSs can handle an unlimited number of EVs. The E-VRP-NL was first introduced by Montoya et al. (2017), who aimed to model a more accurate charging process. The authors propose a piecewise-linear approximation of the charging process and use various charging technologies (e.g. fast, normal, slow). Later, Pelletier et al. (2018) use the same piecewise linear approximation, and consider the electric freight vehicles charge scheduling problem. Froger et al. (2019) propose a path-based model for the E-VRP-NL, which is a more effective alternative model to avoid replicating charging stations. Lee (2021) consider the E-VRP with concave and non-decreasing charging functions. Zhou et al. (2022) consider the electric bus charging scheduling problem with a non-linear charging function and battery degradation effect.

Second, we review the literature assuming that each CS is equipped with only a few chargers and considering the congestion at CSs. Keskin et al. (2019) deal with this issue by explicitly considering expected (i.e., deterministic) time-dependent queuing times at CSs. Kullman et al. (2021) introduce the E-VRP with public-private recharging strategy (E-VRP-PP). They only use a single EV, and consider the non-linear charging functions with a realistic queuing process at the charging station. Froger et al. (2022) extend E-VRP-NL by considering charging station capacity restrictions, leading to the E-VRP-NL-C. Lam et al. (2022) extend E-VRP-NL to the EVRPTW with piecewise-linear recharging and capacitated stations. However, they impose a restriction that there can be at most one charging station visited between any two customers, and only consider a single charging technology. Lera-Romero et al. (2024) combine time-dependent aspects with E-VRP-NL and consider the waiting times at CS. However, they only account for homogeneous EV fleets and assume a uniform waiting time function for all CSs.

2.3. Summary of the E-VRP features and the proposed methods

To provide a clear comparison between our problem and existing studies, we present a summary of the E-VRP features in Table 1. The EV fleet consists of four categories: single vehicle (SV), a homogeneous fleet (HO), a mixed fleet (M), and a heterogeneous fleet (HE). The charging function consists of four types: constant charging time (C), full linear charging (FL), partial linear charging (PL), and non-linear charging (NL). There are two charging technology assumptions: one assumes all CSs are of the same type, and the other assumes each CS may charge at a different speed. There are five approaches to handling congestion at CSs: neglected (NEG), limiting the available chargers at CS (LC), time-dependent waiting time functions (TD), stochastic waiting times (SW), and dynamic decision-making (DYN). Models are categorized into four varieties: replication-based model (Repl),

Table 1: Summary of features in existing E-VRP studies

Reference	Variants	Fleet	Charging function	Multiple Charging	Congestion at CSs	Time Windows	Vehicle Capacity	Model	Method
Erdoğan & Miller-Hooks (2012)	G-VRP	HO	C		NEG			Repl	Heuristics
Schneider et al. (2014)	E-VRPTW	HO	FL		NEG	✓	✓	Repl	VNS/TS
Goeke & Schneider (2015)	E-VRPTWMF	M	PL		NEG	✓	✓	Repl	ALNS
Desaulniers et al. (2016)	E-VRPTW	HO	FL, PL		NEG	✓	✓	SP	Branch-and-price
Hiermann et al. (2016)	E-FSMFTW	HE	FL		NEG	✓	✓	Repl	ALNS
Keskin & Çatay (2016)	E-VRPTW-PR	HO	PL		NEG	✓	✓	Repl	ALNS
Montoya et al. (2017)	E-VRP-NL	HO	NL	✓	NEG			Repl	ILS + HC
Froger et al. (2019)	E-VRP-NL	HO	NL	✓	NEG			Path	MILP solver
Hiermann et al. (2019)	H2E-FTW	M	PL		NEG	✓	✓	–	GA+LNS+SP
Keskin et al. (2019)	EVRPTW	HO	NL		TD	✓	✓	Repl	ALNS
Cortés-Murcia et al. (2019)	E-VRPTWsc	HO	PL		NEG	✓	✓	Repl	ILS+SP
Kullman et al. (2021)	E-VRP-PP	SV	NL	✓	DYN			Repl	Static and dynamic policies
Keskin et al. (2021)	EVRPTW	HO	PL		SW	✓	✓	AF	ALNS
Froger et al. (2022)	E-VRP-NL-C	HO	NL	✓	LC			Path	ILS+branch-and-price
Lam et al. (2022)	EVRPTW-PLR-CRS	HO	NL	✓	LC	✓	✓	Path	Branch-and-cut-and-price
Wang & Zhao (2023)	E-FSMFTW-PR	HE	PL	✓	NEG	✓	✓	Path	LNS+SP
Lera-Romero et al. (2024)	TDEVRPTW	HO	NL	✓	TD	✓	✓	SP	Branch-and-price
Our work	HEVRP-NL	HE	NL	✓	TD	✓	✓	Path	ILS+SP

Fleet: homogeneous fleet (HO), mixed fleet (M), single vehicle (SV), heterogeneous fleet (HE)

Charging function: constant charging time (C), full linear charging (FL), partial linear charging (PL), non-linear charging (NL)

Multiple Charging: each CS may charge at a different speed (e.g., fast, normal, slow)

Congestion at CSs: neglected (NEG), limit the number of charges at CSs (LC), time-dependent waiting time (TD), dynamic decision making (DYN), stochastic waiting time (SW)

Model: replication-based formulation (Repl), path-based formulation (Path), set partitioning with a variable per route (SP), arc-flow formulation (AF)

Methods: Iterated Local Search (ILS), Large Neighborhood Search (LNS), Variable Neighborhood Search (VNS), Genetic Algorithm (GA), Tabu Search (TS)

set-partitioning model (SP), arc-flow model (AF), and path-based model (Path). The meta-heuristics consist of five methods: iterated local search (ILS), large neighborhood search (LNS), variable neighborhood search (VNS), genetic algorithm (GA), and tabu search (TS).

In summary, we consider a heterogeneous fleet of EVs, whose charging process is represented by multiple non-linear charging functions, and we account for time-dependent waiting time functions at CSs.

In terms of models, the path-based formulation (Froger et al., 2019; Wang & Zhao, 2023) has gained popularity in recent years as it does not require duplicating charging stations as in Schneider et al. (2014), Montoya et al. (2017) and Basso et al. (2021). This approach is adopted in this paper. In Section 4, we provide a detailed explanation of how we integrate the features of a heterogeneous fleet, non-linear charging functions, and time-dependent waiting functions into the path-based model.

In terms of meta-heuristics, a combination of local search-based algorithms (GA, ILS, and LNS) with mathematical optimization methods (B&P and SP) has become a powerful approach for solving large-scale E-VRPs in recent years. For the E-VRP-NL, Froger et al. (2022) introduce an ILS algorithm, which has achieved outstanding results. The key to the success of their algorithm lies in their utilization of an exact method to solve a sub-problem named the "fixed route vehicle charging problem (FRVCP)" during the evaluation of local search moves. However, it is important to note that the FRVCP is an NP-hard problem. As a result, when a route contains a significant number of customers, the time required for solving the FRVCP grows exponentially. The difference between our ILS and the ILS described in previous literature lies in the fact that we propose a new route-evaluation function. This function can rapidly evaluate a given sequence of a route under non-linear charging functions when violations of time windows and distance constraints are allowed. Similar to the approach employed by Cortés-Murcia et al. (2019), Hiermann et al. (2019), and Wang & Zhao (2023), we also utilize a set partitioning (SP) model to further enhance the quality of solutions. Our distinguishing feature in this aspect lies in the introduction of a novel route-filtering mechanism that is used to manage the size of the SP model.

3. Problem Description

Our HEVRP-NL problem involves a set of customers C, a set of CS nodes F, and a heterogeneous fleet of EVs denoted by K. Each EV type $k \in K$ has a maximum capacity Q^k, a maximum driving distance Y^k, and a fixed cost f^k. We define $N = C \cup \{0\}$. For each customer $i \in C$, a demand h_i needs to be delivered within the time window $[\alpha_i, \beta_i]$. The service time of each customer is represented by s_i. The travel distance and the travel time between nodes i and j are denoted by d_{ij} and t_{ij}, respectively. EVs can be partially charged at any CS.

We use a partial charging policy, allowing EVs to charge any amount of energy at the CS. Given the presence of different EV types, we extend the non-linear charging functions in Montoya et al. (2017) as follows. Each CS i has a charging technology (e.g., slow, normal, fast) associated with a piecewise linear concave charging function ϕ_{ik} for each EV type k. We denote by $B_{ik} = \{0, \ldots, b_{ik}\}$ the ordered set of breakpoints of the piecewise linear approximation of the charging curve of EV type k at CS i. Let q_{ikm} and c_{ikm} be the State of Charge (SoC, modeled as available driving distance) and the charging time of breakpoint $m \in B_{ik}$ of the EV type k in CS i. Let ρ_{ikm} be the charge slope of the segment joining the breakpoints $(q_{ik,m-1}, c_{ik,m-1})$ and (q_{ikm}, c_{ikm}) (i.e., $\rho_{ikm} = (q_{ikm} - q_{ik,m-1}) / (c_{ikm} - c_{ik,m-1})$) at CS i for EV type k. Figure 1 shows an example of the piecewise linear charging functions for CSs with power of 90kW (fast), 50kW (normal), and 30kW (slow) charging EVs with a 50kWh and a 60kWh battery.

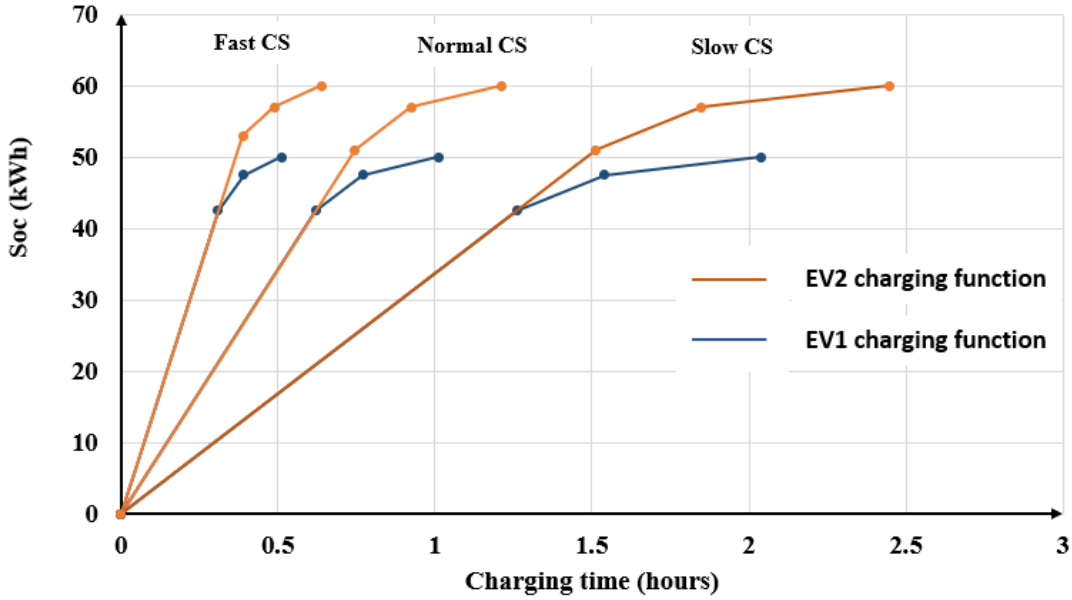

Figure 1: Piecewise linear charging functions for fast CSs, normal CSs, and slow CSs charging EV1 with 50kWh battery and EV2 with 60kWh battery

Since each CS is equipped with a limited number of chargers, EVs may need to wait in line before they can be charged. We adopt non-linear waiting time functions and approximate them using piecewise linear functions as in Keskin et al. (2019). The waiting time functions satisfy the FIFO property. It is assumed that the expected waiting time at all CSs and at any given arrival time can be estimated in advance (e.g., from the historical data or drivers' experience). Thus, each CS i has a piecewise linear time-dependent waiting time function $W_i(t)$ when an EV arrives at a CS at any time t. We denote by $\mathcal{M}_i = \{0, \ldots, M_i\}$ the ordered set of time intervals of the $W_i(t)$ function at CS i. Let W_i^m be the waiting time at CS i at the beginning of m^{th} time interval, S_i^m be the slope of the waiting time function of CS i in m^{th} time interval, and A_i^m be the time length of the m^{th} time interval at CS i. Figure 2 shows an

example of the piecewise linear time-dependent waiting time functions for CSs.

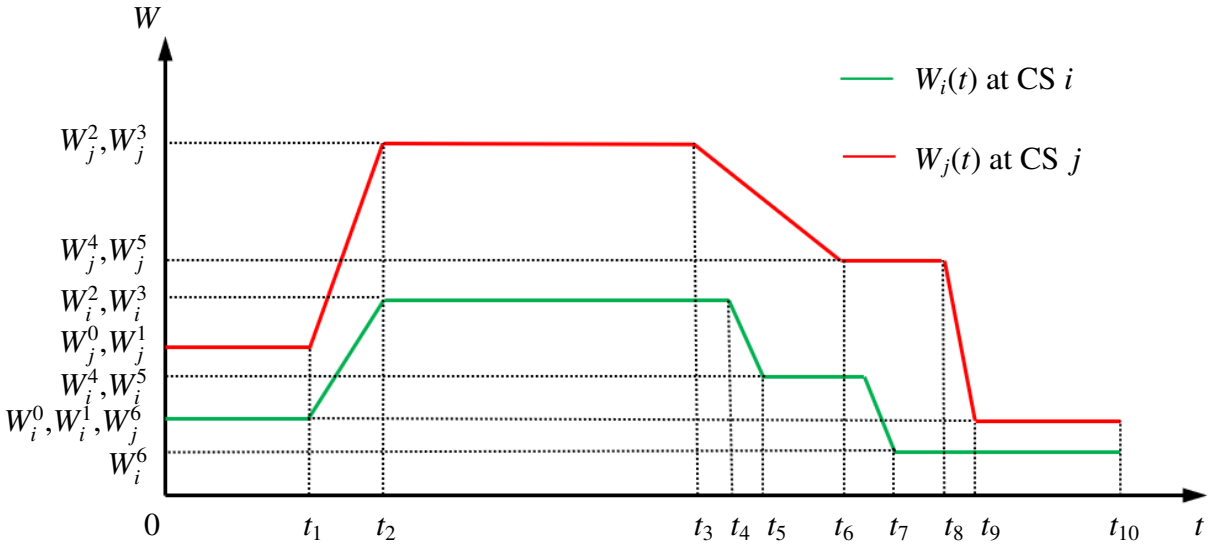

Figure 2: Piecewise linear time-dependent waiting time functions according to Keskin et al. (2019)

A feasible solution must satisfy the following conditions: 1) each customer is visited exactly once by an EV; 2) each route starts and ends at the depot; 3) each route is feasible with respect to energy, time windows, and capacity constraints. The objective of the HEVRP-NL is to minimize the sum of travel time costs, charging time costs, and fixed costs. The first term is the sum of the total travel time of all trips, the second term is the sum of charging time at each CS, and the third term is the sum of the costs of all activated EVs.

4. A mixed-integer linear programming model

4.1. Path-Based Model

Most of the existing models for E-VRPs can be classified into two categories: replication-based models and path-based models. To allow multiple visits to each CS, many studies (Schneider et al. (2014), Keskin & Çatay (2016),Hiermann et al. (2016), Montoya et al. (2017), Kullman et al. (2021)) replicate the CSs in the mathematical model. These models need to set the number of copies of each charging station, which greatly increases the solution time. To avoid replicating CS nodes, other studies use a more complex but more effective approach, named the path-based model. Their idea is either to enumerate paths of visits to CSs between any two customer nodes or depot nodes (Roberti & Wen (2016), Andelmin & Bartolini (2017), Froger et al. (2019), Froger et al. (2022)), or enumerate paths of visits to customers between any two CSs or the depot (Bruglieri et al. (2019a), Bruglieri et al. (2019b)). We refer to the former case as CS paths and to the latter as customer paths.

In this paper, we propose a path-based model based on CS paths for the following reasons: a) the number of customer paths grows much faster than the number of CS paths; b) customer path-based

formulations require introducing a sufficient number of copies of paths that do not visit any customer between two charging stations.

4.2. Path Enumeration

The idea of the CS path-based model is to enumerate all paths between any two non-charging nodes. We refer to this set of paths as P. The set P_{ijk} comprises paths from node $i \in N$ to node $j \in N$ by EV type $k \in K$. Note that this concept of path is adopted from Froger et al. (2019), and paths from i to j may include one or multiple visits to CSs, without including any customers. We define parameters $org(p) = i$, $dest(p) = j$, and $evt(p) = k$, which represent the starting node, destination node, and EV type of path p. Let d_p be the travel distance of path p. The value t_p represents the travel time of path p without considering charging time or waiting time at CS. Let $n(p)$ be the number of CSs on path p. If $n(p) = 0$, it means there are no CSs visited on path p, i.e., the EV travels directly from node $org(p)$ to node $dest(p)$. We define $cs(p, l)$ as the l-th CS on path p ($l \in \{1 \dots n(p)\}$). Let τ_{plm} ($m \in B_{cs(p,l)k} = \left\{0, \dots, b_{cs(p,l)k}\right\}$) be the charge distance of the segment joining the breakpoints $m-1$ and m at CS $cs(p, l)$ on path P_{ijk}. Thus, $\tau_{plm} = q_{cs(p,l)km} - q_{cs(p,l)k,m-1}$.

Even with the CS path-based model, the number of paths can still be very large. Given k EV types, m charging stations, and n non-recharging nodes, the time complexity of enumeration is $O(k \cdot n^2 \cdot m!)$. To overcome this, we eliminate infeasible paths by applying constraint conditions (refer to Section 4.3), and design dominance rules for CSs to eliminate dominated paths (refer to Section 4.4) to make our model more tractable.

4.3. Eliminating infeasible paths

To reduce the size of the path set P, we employ the following constraints (1)-(3) to eliminate infeasible paths without affecting the optimal solution.

Constraints (1) check if a path p violates the time window. If so, the path can be eliminated. The value of ρ^* is the steepest slope for a segment of the piece-wise linear charging functions on path p (i.e., $\rho^* = max_{l=1\dots n(p)}\{\rho_{cs(p,l)1}\}$). $W_{min}^{cs(p,l)}$ represents the minimum waiting time of each CS on path p. Under the condition of performing the minimum charging time and minimum waiting time, the EV would arrive beyond the latest arrival time of the ending node:

$$\alpha_{org(p)} + s_{org(p)} + t_p + max\{0, d_p - Q^{evt(p)}\}/\rho^* + \sum_{l=1}^{n(p)} W_{min}^{cs(p,l)} > \beta_{dest(p)} \qquad \forall p \in P, n(p) > 0. \tag{1}$$

Constraints (2) check if a path p violates the distance constraint. If so, the path can be eliminated. It means that when the EV traverses this path, the SoC is insufficient to reach the nearest CS or return

to the depot:

$$\min_{l \in F \cup \{0\}} \{d_{li}\} + d_{ij} + \min_{l \in F \cup \{0\}} \{d_{il}\} > Y^{evt(p)} \qquad \forall i, j \in C, k \in K, n(p) = 0, p \in P_{ijk}. \tag{2}$$

Constraints (3) check if a path p violates the capacity constraint. If so, the path can be eliminated. It means that the capacity on that path exceeds the maximum load capacity of the EV:

$$h_{org(p)} + h_{dest(p)} > Q^{evt(p)} \qquad \forall p \in P. \tag{3}$$

4.4. Eliminating dominated paths

After eliminating the infeasible paths, we proceed to eliminate the dominated paths. A path p that involves no CS (i.e., $n(p) = 0$) cannot be dominated by other paths. As for a path p that contains at least one CS (i.e., $n(p) \geq 1$), we define it as a Recharging Path (RP). By designing the dominance rule, we eliminate the dominated RPs.

For an RP p, let $\overline{\phi_p}$ and $\underline{\phi_p}$ as the charging functions corresponding to the fastest and slowest CS on path p. Let $\overline{W_p}$ and $\underline{W_p}$ as the waiting time functions corresponding to the busiest and least busy CSs on path p. Let t_p^{org} as the travel time from the starting node to the first CS on path p. Let t_p^{dest} be the travel time from the last CS to the destination node on path p.

Dominance Rule: Let an RP $p1$ and another RP $p2$ have the same starting node $org(p1) = org(p2) = o$ and the same ending node $dest(p1) = dest(p2)$. We can eliminate the dominated RP $p2$ if the following conditions are met: 1) the charging rate of $\underline{\phi_{p1}}$ is equal to or faster than $\overline{\phi_{p2}}$; 2) the waiting time of $\underline{W_{p1}}$ is equal to or shorter than the waiting time of $\overline{W_{p2}}$ at any time interval; 3) $(t_{p1}^{org} \leq t_{p2}^{org}) \wedge (t_{p1}^{dest} \leq t_{p2}^{dest}) \wedge (d_{p1} \leq d_{p2})$.

4.5. Formulation

We define the decision variables as follows. The binary variable x_p takes the value 1 if path p is selected, and 0 otherwise. The continuous variables a_p, $\hat{h}_p$, and r_p track the time, capacity, and remaining travel distance of EV arrival on path p, respectively. The continuous variable Δ_{pl} tracks the charging time of the l-th CS on path p. The continuous variables $\underline{y}_{pl}$ and $\overline{y}_{pl}$ track the remaining travel distance when EV enters and leaves CS $cs(p, l)$. For $m \in B_{cs(p,l)k}$, the binary variables $\underline{w}_{plm}$ and $\overline{w}_{plm}$ represent whether the SoC is larger than $q_{cs(p,l)k,m-1}$ when EV enters and leaves CS $cs(p, l)$; the continuous variables $\underline{\lambda}_{plm}$ and $\overline{\lambda}_{plm}$ represent the coefficients associated with the segment charging distance τ_{plm} when EV enters and leaves CS $cs(p, l)$. The continuous variable Λ_{pl} represents the waiting time at the l-th CS on path p. The continuous variable u_{pl} tracks the EV's arrival time at the l-th CS on path p. The binary variable δ_{plm} takes the value of 1 if the EV's arrival time at the l-th

CS on path p is larger than the arrival time at the beginning of m^{th} time interval, and 0 otherwise. The continuous variable z_{plm} represents the coefficients associated with the time length of the m^{th} time interval at the l-th CS on path p. The path-based formulation of the HEVRP-NL is as follows:

$$\min \sum_{p\in P}\left(x_p t_p + \sum_{l=1}^{n(p)} \Delta_{pl}\right) + \sum_{j\in N,k\in K,p\in P_{0jk}} x_p f^{evt(p)} \tag{4}$$

$$\text{s.t.} \sum_{j\in N,k\in K,p\in P_{ijk}} x_p = 1 \qquad \forall i \in C \tag{5}$$

$$\sum_{j\in N,p\in P_{ijk}} x_p = \sum_{j\in N,p\in P_{jik}} x_p \qquad \forall i \in C, \forall k \in K \tag{6}$$

$$\sum_{j\in N,k\in K,p\in P_{ijk}} x_p = \sum_{j\in N,k\in K,p\in P_{jik}} x_p \qquad \forall i \in N \tag{7}$$

$$\sum_{j\in N,k\in K,p\in P_{jik}} \hat{h}_p = \sum_{j\in N,k\in K,p\in P_{ijk}} \hat{h}_p + h_i \qquad \forall i \in C. \tag{8}$$

The objective function (4) minimizes the sum of travel time cost, charging time cost, and fixed cost. Constraints (5) ensure that each customer is visited exactly once. Constraints (6) ensure that the EV type for visiting each customer is consistent with the EV type for leaving each customer. Constraints (7) ensure that EVs must leave after visiting customers, and EVs departing from the depot center must return to the depot center. Constraints (8) track the load capacity of EVs when they visit each customer.

Time Window Constraints:

$$\sum_{j\in N,k\in K,p\in P_{jik}} (a_p + x_p(t_p + s_i) + \sum_{l=1}^{n(p)} (\Delta_{pl} + \Lambda_{pl})) = \sum_{j\in N,k\in K,p\in P_{ijk}} a_p \quad \forall i \in C \tag{9}$$

$$a_p + x_p t_p + \sum_{l=1}^{n(p)} (\Delta_{pl} + \Lambda_{pl}) \le \beta_0 \qquad \forall i \in C, k \in K, p \in P_{i0k} \tag{10}$$

$$x_p \alpha_i \le a_p - x_p s_i \le x_p \beta_i \qquad \forall i \in C, j \in N, k \in K, p \in P_{ijk}. \tag{11}$$

Constraints (9) enforce that the departure time of the EV from each customer $i = dest(p)$ on path p is equal to the sum of the departure time of the EV from $org(p)$, the travel time on path p, the total charging time on path p, and the service time at i. Constraints (10) ensure that the return time of the EV to the depot does not exceed its latest time. Constraints (11) ensure that the time windows of all customers are satisfied.

Distance Constraints:

$$\underline{y}_{pl} \le \overline{y}_{pl} \qquad \forall p \in P \tag{12}$$

$$r_p - x_p d_{org(p),cs(p,1)} = \underline{y}_{p1} \qquad \forall p \in P \tag{13}$$

$$\overline{y}_{p,l-1} - x_p d_{cs(p,l-1),cs(p,l)} = \underline{y}_{pl} \qquad \forall p \in P, l = \{2, \ldots, n(p)\} \tag{14}$$

$$\sum_{j \in N, k \in K, p \in P_{jik}} (r_p - x_p d_p + \sum_{l=1}^{n(p)} (\overline{y}_{pl} - \underline{y}_{pl})) = \sum_{j \in N, k \in K, p \in P_{ijk}} r_p \qquad \forall i \in C \tag{15}$$

$$r_p - x_p d_p + \sum_{l=1}^{n(p)} (\overline{y}_{pl} - \underline{y}_{pl}) \geq 0 \qquad \forall i \in C, k \in K, p \in P_{i0k}. \tag{16}$$

Constraints (12) ensure that the SoC of the EV upon arrival at each CS is less than or equal to the SoC of the EV upon departure from the CS. For each path p, Constraints (13) ensure that the EV has enough travel distance to reach the first CS. Constraints (14) express the SoC relationship of the EV between two consecutive CSs on path p. Constraints (15) track the SoC of EV when it visits each customer. Constraints (16) ensure that the EV has enough SoC to return to the depot.

Non-Linear Charging Function:

$$\underline{y}_{pl} = \sum_{m \in B_{cs(p,l),evt(p)}} \underline{\lambda}_{plm} \tau_{plm} \qquad \forall p \in P, l = 1, \ldots, n(p) \tag{17}$$

$$\underline{w}_{plm} \geq \underline{w}_{pl,m-1} \qquad \forall p \in P, l = 1, \ldots, n(p), m = 1, \ldots, b_{cs(p,l),evt(p)} \tag{18}$$

$$\underline{w}_{plm} \geq \underline{\lambda}_{plm} \geq \underline{w}_{pl,m+1} \qquad \forall p \in P, l = 1, \ldots, n(p), m = 0, \ldots, b_{cs(p,l),evt(p)} - 1 \tag{19}$$

$$\overline{y}_{pl} = \sum_{m \in B_{cs(p,l),evt(p)}} \overline{\lambda}_{plm} \tau_{plm} \qquad \forall p \in P, l = 1, \ldots, n(p) \tag{20}$$

$$\overline{w}_{plm} \geq \overline{w}_{pl,m-1} \qquad \forall p \in P, l = 1, \ldots, n(p), m = 1, \ldots, b_{cs(p,l),evt(p)} \tag{21}$$

$$\overline{w}_{plm} \geq \overline{\lambda}_{plm} \geq \overline{w}_{pl,m+1} \qquad \forall p \in P, l = 1, \ldots, n(p), m = 0, \ldots, b_{cs(p,l),evt(p)} - 1 \tag{22}$$

$$\Delta_{pl} = \sum_{m \in B_{cs(p,l),evt(p)}} \overline{\lambda}_{plm} \tau_{plm} / \rho_{cs(p,l),evt(p),m} - \sum_{m \in B_{cs(p,l),evt(p)}} \underline{\lambda}_{plm} \tau_{plm} / \rho_{cs(p,l),evt(p),m} \qquad \forall p \in P, l = 1, \ldots, n(p). \tag{23}$$

Constraints (17) - (19) track the SoC of the EV upon arrival at each CS. Constraints (20) - (22) track the SoC of the EV upon departure from each CS. Constraints (23) express the non-linear charging function (piece-wise linear function) between the charging distance and the charging time for each CS.

Time-Dependent Waiting Time Function:

$$u_{pl} = \sum_{m \in \mathcal{M}_{cs(p,l)}} z_{plm} A^m_{cs(p,l)} \qquad \forall p \in P, l = 1, \ldots, n(p) \tag{24}$$

$$\delta_{plm} \geq \delta_{pl,m-1} \qquad \forall p \in P, l = 1, \ldots, n(p), m = 1, \ldots, M_{cs(p,l)} \tag{25}$$

$$\delta_{plm} \geq z_{plm} \geq \delta_{pl,m+1} \qquad \forall p \in P, l = 1, \ldots, n(p), m = 0, \ldots, M_{cs(p,l)} - 1 \quad (26)$$

$$\Lambda_{pl} = x_p W^0_{cs(p,l)} + \sum_{m \in \mathcal{M}_{cs(p,l)}} z_{plm} A^m_{cs(p,l)} S^m_{cs(p,l)} \qquad \forall p \in P, l = 1, \ldots, n(p) \quad (27)$$

$$u_{pl} \geq u_{p,l-1} + \Lambda_{p,l-1} + \Delta_{p,l-1} + x_p t_{cs(p,l-1),cs(p,l)} \qquad \forall p \in P, l = 2, \ldots, n(p) \quad (28)$$

$$u_{p1} \geq a_p + x_p t_{org(p),cs(p,1)} \qquad \forall p \in P. \quad (29)$$

Constraints (24) - (26) track the arrival time of EV at each CS. Constraints (27) track the waiting time of EV at each CS. Constraints (28) - (29) describe the relationship between the arrival time of EV at each CS and the arrival time of the EV at the preceding node.

Domains of the Decision Variables:

$$x_p \in \{0, 1\} \qquad \forall p \in P \quad (30)$$

$$0 \leq \hat{h}_p \leq x_p Q^{evt(p)} \qquad \forall p \in P \quad (31)$$

$$0 \leq a_p \leq x_p \beta_0, 0 \leq \sum_{l=1}^{n(p)} (\Lambda_{pl} + \Delta_{pl}) \leq x_p \beta_0 \qquad \forall p \in P \quad (32)$$

$$0 \leq r_p \leq x_p Y^{evt(p)} \qquad \forall p \in P, l = 1, \ldots, n(p) \quad (33)$$

$$0 \leq \underline{y}_{pl} \leq x_p Y^{evt(p)}, 0 \leq \overline{y}_{pl} \leq x_p Y^{evt(p)} \qquad \forall p \in P, l = 1, \ldots, n(p) \quad (34)$$

$$0 \leq u_{pl} \leq x_p \beta_0 \qquad \forall p \in P, l = 1, \ldots, n(p) \quad (35)$$

$$\overline{w}_{plm} \in \{0, 1\}, \underline{w}_{plm} \in \{0, 1\} \qquad \forall p \in P, l = 1, \ldots, n(p), m \in B_{cs(p,l),evt(p)} \quad (36)$$

$$0 \leq \underline{\lambda}_{plm} \leq 1, 0 \leq \overline{\lambda}_{plm} \leq 1 \qquad \forall p \in P, l = 1, \ldots, n(p), m \in B_{cs(p,l),evt(p)} \quad (37)$$

$$\delta_{plm} \in \{0, 1\}, 0 \leq z_{plm} \leq 1 \qquad \forall p \in P, l = 1, \ldots, n(p), m \in \mathcal{M}_{cs(p,l)}. \quad (38)$$

Constraints (30) define variables x_p as 0-1 binary variables that represent whether path p is visited. Constraints (31) force $\hat{h}_p$ to 0 if the EV does not visit path p. Constraints (32) force a_p, Λ_{pl} and Δ_{pl} to 0 if the EV does not visit path p. Constraints (33) - (35) forcibly assign r_p, u_{pl}, $\underline{y}_{pl}$ and $\overline{y}_{pl}$ as 0 if the EV does not visit path p. Constraints (36) - (38) define the domain of the decision variables $\underline{w}_{plm}$, $\overline{w}_{plm}$, $\underline{\lambda}_{plm}$, $\overline{\lambda}_{plm}$, δ_{plm} and z_{plm}.

5. Solution Method

In recent years, a combination of local search-based algorithms with mathematical optimization methods has become a powerful approach for solving large-scale E-VRPs, such as Hiermann et al. (2019), Cortés-Murcia et al. (2019), Froger et al. (2022) and Wang & Zhao (2023). In this paper, we present an algorithm that decomposes the HEVRP-NL into a route generation-based problem and

a route assembler-based problem. Thus, the algorithmic framework consists of two components: a route generator and a route assembler as described in Algorithm 1. The route assembler is a set partitioning model, which is efficient to solve, and this mechanism allows us to deal with the complex constraints of each route in a flexible and efficient manner.

The first component employs an iterated local search algorithm equipped with a problem-specific route evaluation function. Starting from an initial solution S, this part of the algorithm finds the local optimal solution $S^{'}$ and adds high-quality routes to the pool Ω. The second component employs a set-partitioning model to combine a subset of routes from the pool Ω into a new solution $S^{''}$. At the end of each iteration, we update the best feasible solution S_{best}. The algorithmic framework iterates between these two components.

We allow violations in capacity, time window, and distance constraints, by making use of penalty parameters λ, η_{fea} and η_{infea} to guide the algorithm's search between feasible and infeasible solution spaces. The parameter λ represents the penalty factor, with an initial value of λ_0. The parameters η_{fea} and η_{infea} represent the number of consecutive iterations with feasible solutions and infeasible solutions, respectively.

Algorithm 1 The algorithmic framework

$S_{\text{best}} \leftarrow \phi$, $\Omega \leftarrow \phi$, $\lambda \leftarrow \lambda_0$, $\eta_{\text{fea}} \leftarrow 0$, $\eta_{\text{infea}} \leftarrow 0$
$n \leftarrow 1$
Construct an initial solution S
while $n \leq n^{max}$ **do**
  $S^{'} \leftarrow GenerateRoutes(S, \lambda, \eta_{\text{fea}}, \eta_{\text{infea}})$ ····· Route Generator (see Algorithm 2)
  $S^{''} \leftarrow AssembleRoutes(S^{'}, \Omega, n)$ ····· Route Assembler (see Algorithm 5)
  if $S^{''}$ is a feasible solution and $S^{''}$ is better than S_{best} **then**
    $S_{\text{best}} \leftarrow S^{''}, S \leftarrow S^{''}$
  end if
  $n \leftarrow n + 1$
end while
return S_{best}

5.1. Route Generator

We first perturb the current solution S by employing destroy-and-repair operators to improve the solution diversity and escape from local optima. Then, we utilize a variable neighborhood descent (VND) procedure to obtain a local optimal solution $S^{'}$. Finally, we check the feasibility of $S^{'}$ and update the penalty parameters. Specifically, after η_{penalty} consecutive iterations with violated constraints, λ is multiplied by a factor of ε. Conversely, if all the constraints are satisfied for η_{penalty} consecutive iterations, λ is divided by ε. Algorithm 2 presents the route generator.

Algorithm 2 The Route Generator - *GenerateRoutes*$(S, \lambda, \eta_{\text{fea}}, \eta_{\text{infea}})$

Parameters: η_{penalty}, ε
$S \leftarrow Perturbation(S, \lambda)$
$S' \leftarrow VND(S, \lambda)$
if S' is a feasible solution **then**
  $\eta_{\text{fea}} \leftarrow \eta_{\text{fea}} + 1, \eta_{\text{infea}} \leftarrow 0$
else if S' is an infeasible solution **then**
  $\eta_{\text{infea}} \leftarrow \eta_{\text{infea}} + 1, \eta_{\text{fea}} \leftarrow 0$
end if
if $\eta_{\text{infea}} \geq \eta_{\text{penalty}}$ **then**
  $\lambda \leftarrow \lambda * \varepsilon, \eta_{\text{infea}} \leftarrow 0$
else if $\eta_{\text{fea}} \geq \eta_{\text{penalty}}$ **then**
  $\lambda \leftarrow \lambda / \varepsilon, \eta_{\text{fea}} \leftarrow 0$
end if
$UpdateSolution(S', \lambda)$
return S'

5.1.1. Solution Evaluation and Generalized Cost Function

Given a route r of EV type k, which includes a sequence of customers and CSs, we define a generalized cost function (39) to evaluate it. The parameters $f_{\text{tc}}(r)$, $f_{\text{fc}}(r)$ and $f_{\text{cc}}(r)$ represent the travel time cost, fixed cost and charging time cost of route r, respectively. The sum of these three terms represents the original objective function. The parameters $P_{\text{Cap}}(r)$, $P_{\text{TW}}(r)$, and $P_{\text{Dis}}(r)$ are the violations of capacity, time window, and distance constraints, respectively. The details of the route evaluation are shown in Section 5.1.2. We obtain the following cost function:

$$f^k_{\text{gen}}(r) = f_{\text{tc}}(r) + f_{\text{fc}}(r) + f_{\text{cc}}(r) + \lambda \left(P_{\text{Cap}}(r) + P_{\text{TW}}(r) + P_{\text{Dis}}(r) \right). \tag{39}$$

Next, we evaluate each route r under each vehicle type $k \in K$ and select the optimal EV type with the routing cost $f_{\text{best}}(r)$ by the function (40):

$$f_{\text{best}}(r) = \min_{k \in K} f^k_{\text{gen}}(r). \tag{40}$$

Finally, a solution S is defined as a set of n routes represented as $S = \{r_1, \ldots, r_n\}$ and can be evaluated by using the generalized cost function (41):

$$f_{\text{gen}}(S) = \sum_{i=1}^{n} f_{\text{best}}(r_i). \tag{41}$$

5.1.2. Route Evaluation

This section is devoted to evaluating a given route r of EV type k with a sequence of customers and CSs by computing its minimum cost function (39). For a given route r, travel time cost $f_{\text{tc}}(r)$,

fixed cost $f_{\text{fc}}(r)$ and capacity violation $P_{\text{Cap}}(r)$ are easy to compute, with a computational complexity of $O(1)$. Thus, to minimize the routing cost is to minimize the sum of charging time cost $f_{\text{cc}}(r)$, time-window violation $P_{\text{TW}}(r)$ and distance violation $P_{\text{Dis}}(r)$, which is a challenging problem since this information cannot be known in advance.

Suppose we have a route containing four customers and two CSs, which is shown in Fig 3. If the EV departs from the depot at the earliest time, serves each customer, and travels without charging or waiting at any CS, the time vectors of the route are shown in Fig 3 (a). Note that since the charging time cost only exists at CS, we can further obtain the simplified time vectors between the depot and CS nodes as shown in Fig 3 (b). When the EV is waiting or charging at a CS, the time vector at the CS will shift to the right. Therefore, we can have the following observation.

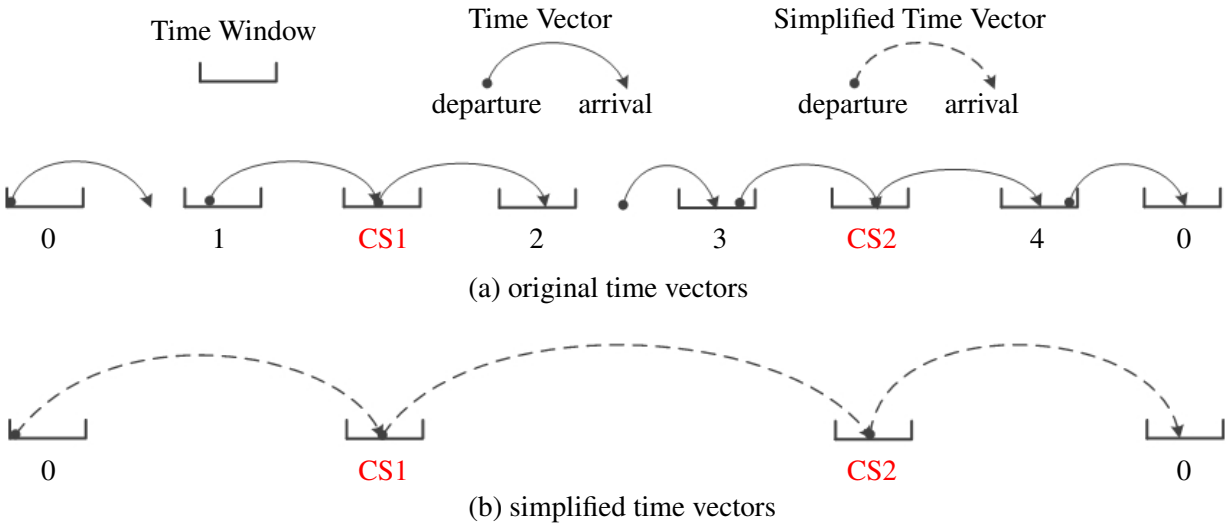

Figure 3: An example of time vectors for a route without charging or waiting at any CS

Observation: For a certain route r of EV type k, where the EV traverses without charging or waiting at any CS, our goal is to shift the time vectors of CSs as little as possible to meet the time window and distance constraints.

We employ a heuristic algorithm that follows a "minimize charging time first and minimize waiting time second" strategy. The strategy consists of three steps. In the first step, the EV follows a "no charging, no waiting" strategy along the route. In the second step, we shift the time vectors of CSs to perform the charging time as minimally as possible to satisfy distance constraints. In the third step, we determine the waiting time at each CS.

Step1: EV (fully charged) traverses route r with a condition of "no charging or waiting" at CS.

Under this condition, we obtain the arrival time a_i and the leave time l_i for each node i. If this condition leads to a violation of the time window at a node, we incorporate the violation into $P_{\text{TW}}(r)$ and force the node's arrival time back to the end of its time window. Then, we define the CS node and depot node as non-customer nodes. For each non-customer node i, we define the variables T_i^{max},

T_i^{slack}, T_i^{arr}, q_i^{arr}, q_i^{lea}, T_i^C, T_i^D and T_i^W. These variables are initialized as follows:

$$T_i^{max} = \beta_i - a_i \tag{42}$$

$$T_i^{slack} = \sum_{n=i}^{j} \max\{0, \alpha_n - a_n\} \tag{43}$$

$$T_i^{arr} = a_i \tag{44}$$

$$q_i^{arr} = q_i^{lea} = Y^k - \sum_{n=1}^{i} d_{n-1,n} \tag{45}$$

$$T_i^C = 0 \tag{46}$$

$$T_i^D = 0 \tag{47}$$

$$T_i^W = W_i(T_i^{arr}). \tag{48}$$

The variable T_i^{max} represents the maximum shift time at node i without violating its time window, which is initialized in Expression (42). The variable T_i^{slack} represents the sum of the waiting times of customers between node i and the next non-customer node j, which is initialized in Expression (43). The variable T_i^{arr} represents the arrival time at node i, which is initialized in Expression (44). The maximum driving distance of EV type k is Y^k, the variables q_i^{arr} and q_i^{lea} represent the SoC when the EV arrives and leaves node i, respectively, which are initialized in Expression (45). The variables T_i^C and T_i^D represent the charging time and the duration of delay time in reaching node i, which are initialized in Expressions (46) and (47). The variable T_i^W represents the waiting time at node i, which is initialized in Expression (48).

We obtain the simplified route $r = \{0, CS_1, CS_2, \ldots, CS_n, 0\}$, which only contains the depot node and n CS nodes (where n may be 0).

Step2: Shifting the time vectors of CSs to minimize the charging time.

Our task is to minimize the total charging time cost by determining the charging time T_i^C at each CS node i. The method is shown in Algorithm 3. We sequentially examine q_i^{arr} at each CS i in order. We begin with the first non-customer node with a negative q_i^{arr}. It indicates that the EV does not have enough available driving distance to reach node i, and the EV needs to charge at CSs before node i to ensure a non-negative SoC upon arrival.

Since different CSs have different non-linear charging functions, we assess the SoC of the EV at each CS before node i to obtain the corresponding charging slope. We select the CS c with the steepest charging slope ρ_c as the fastest CS. Next, we calculate the maximum available charging time T_c^{charge} at the charging rate of ρ_c. We add T_c^{charge} to T_i^C and perform T_c^{charge} at CS c. Such charging operations will be repeated until q_i^{arr} becomes 0, then we continue to examine the SoC of the next

non-customer node.

Algorithm 3 Minimize the Total Charging Time

for $i \in \{0, CS_1, CS_2, \ldots, CS_n, 0\}$ **do**
  if $q_i^{arr} < 0$ **then**
    while $q_i^{arr} < 0$ **do**
      $c \leftarrow Find\_Fastest\_Available\_CS(i)$
      if c is null **then**
        $P_{\text{Dis}}(r) \leftarrow P_{\text{Dis}}(r) - q_i^{arr}$
        for $j \in \{CS_i, \ldots, CS_n, 0\}$ **do**
          $q_j^{arr} \leftarrow q_j^{arr} - q_i^{arr}$,$q_j^{lea} \leftarrow q_j^{lea} - q_i^{arr}$
        end for
      else
        $T_c^{charge} \leftarrow Get\_Max\_Charging\_Time(c, -q_i^{arr})$ ····· (see Algorithm 6)
        $T_c^C \leftarrow T_c^C + T_c^{charge}$
        $PerformChargeTime(c, T_c^{charge})$ ····· (see Algorithm 9)
      end if
    end while
  end if
end for

However, when it is impossible to find a CS before node i that can be used for charging, q_i^{arr} remains negative. This implies that, no matter how much charging takes place at CSs before node i, the EV will not have enough energy to reach node i. In such cases, we add q_i^{arr} to $P_{\text{Dis}}(r)$, and we forcefully replenish $-q_i^{arr}$ of SoC for each subsequent node after node i.

The above charging operation will continue until the last non-customer node is examined.

Step3: Shifting the time vectors of CSs to perform the waiting time.

Since the waiting time functions satisfy the FIFO property, delaying the departure time cannot improve the solution. After charging in **Step2**, we proceed to perform waiting time at each CS based on the time-dependent waiting time function. The details are shown in Algorithm 4.

5.1.3. Initial solution

We construct the initial solution by using a combination of a greedy insertion criterion and a random factor. We begin by having the vehicle start from the depot and randomly select an unassigned customer as the first customer to be served. The remaining part is to insert the rest of the unassigned customers at the position that minimally increases the objective function (41). Note that we allow the creation of a new route to serve a customer. This process continues iteratively until all customers have been assigned to routes and there are no remaining unassigned customers.

5.1.4. Perturbations

We remove κ customers from their respective routes, with κ randomly selected in the interval $[\min\{|C|, 3\}, \max\{\min\{|C|, 3\}, [\sqrt{|C|}\,|]\}]$. We use the following destroy operators:

Algorithm 4 Perform the Waiting Time

for $c \in \{CS_1, CS_2, \ldots, CS_n\}$ **do**
  $T^{wait} \leftarrow T_c^W$
  for $i \in \{CS_c, \ldots, CS_n, 0\}$ **do**
    if $i \neq c$ **then**
      $T_i^{arr} \leftarrow T_i^{arr} + T^{wait}$
    end if
    $T_i^{shift} \leftarrow Get\_Max\_Shift\_Time(i)$ ····· (see Algorithm 8)
    if $T_i^{shift} < T^{wait}$ **then**
      $P_{\mathrm{TW}}(r) \leftarrow P_{\mathrm{TW}}(r) + T^{wait} - T_i^{shift}$
      $T^{wait} \leftarrow T_i^{shift}$
    end if
    $T_i^{max} \leftarrow T_i^{max} - T^{wait}$
    $T^{temp} \leftarrow T^{wait}$
    $T^{wait} \leftarrow Max(0, T^{wait} - T_i^{slack})$
    $T_i^{slack} \leftarrow Max(0, T_i^{slack} - T^{temp})$
    if $T^{wait} = 0$ **then**
      break
    end if
  end for
  for $i \in \{CS_c, \ldots, CS_n\}$ **do**
    $T_i^W \leftarrow W_i(T_i^{arr})$
  end for
end for

Closest Removal: We randomly select a customer $i \in C$ and remove the $\kappa - 1$ "closest" customers to i from their respective routes. We use the customer correlation function (49) of Vidal et al. (2013) to calculate how "close" two customers are to each other:

$$r(i,j) = d_{ij} + r^{WT} \max\left(\alpha_j - s_i - t_{ij} - \beta_i, 0\right) + r^{TW} \max\left(\alpha_i + s_i + t_{ij} - \beta_j, 0\right), \tag{49}$$

where $[\alpha_i, \beta_i]$ and s_i represent the time window and service time of customer i, respectively. Additionally, r^{WT} and r^{TW} represent the coefficients for unavoidable waiting time and time window violation.

Random Removal: We randomly select κ customers for removal.

The repair operators are as follows:

Greedy Insertion: We insert a node into the best position according to function (41) using the best insertion policy.

2-Regret Insertion: We use a regret value to determine which node to insert based on the difference between the best and second-best insertion positions.

The above operations are used with uniform probability.

5.1.5. Variable neighborhood descent – VND

The VND is implemented as a local search strategy following the best improvement strategy. We apply six neighborhood operations: Intra-Swap, Inter-Swap, Intra-Relocate, Inter-Relocate, Tail-Cross, and a problem-specific operator called **ReplacePath**. The swap operator generates a neighborhood solution by randomly swapping the positions of two different customers. The relocate operator randomly selects two customers (i, j), removes customer i from its original route and inserts it before or after customer j. The tail-cross operator selects two customers (i, j) randomly from two different routes (Route1 and Route2). Then, we interchange the node after customer i in Route 1 with the node after customer j in Route 2.

To efficiently manage the CSs, we introduce the **ReplacePath** operator, which is tailored to our problem. Note that we can enumerate all feasible non-dominated paths between any two non-charging nodes, as detailed in Section 4. The **ReplacePath** operator randomly selects a path p from the current solution. Subsequently, we randomly select another path p' that has the same origin and destination nodes as p, and replace p with p'.

5.2. Route Assembler

The idea behind the Route Assembler is to store the generated routes in a pool and to formulate a set partitioning (SP) model to obtain a new solution. This method has the following two issues: a) the time required to solve the SP model will grow exponentially as the number of routes in the pool increases, so it is necessary to control the size of the pool properly; b) due to limited storage space, it is not possible to include all generated routes in the pool. Therefore, when the pool is full, a filtering mechanism is needed to decide which routes are added or removed.

5.2.1. Set Partitioning Model

Let Ω be the pool of feasible routes. The 0-1 binary variable θ_r represents whether route r is included in the solution or not. The parameter c_r is the routing cost of each $r \in \Omega$. The 0-1 binary parameter ψ_{ir} represents whether route r visits customer i. The HEVRP-NL can be formulated as the following SP model:

$$\min \sum_{r \in \Omega} c_r \theta_r \tag{50}$$

$$\text{s.t.} \sum_{r \in \Omega} \psi_{ir} \theta_r = 1 \qquad \forall i \in C \tag{51}$$

$$\theta_r \in \{0, 1\} \qquad \forall r \in \Omega. \tag{52}$$

A linear programming (LP) relaxation of the SP can be formulated by relaxing the binary variables

θ_r to continuous variables. By solving the LP, the values of the dual variable π_i ($i \in C$) associated with constraints (51) are obtained. Let χ_r be the reduced cost of route r as follows:

$$\chi_r = c_r - \sum_{i \in C} \pi_i \psi_{ir}. \tag{53}$$

5.2.2. Managing the Pool

To restrict the memory usage and computational effort, the size of the pool Ω is bounded by ξ. A filtering mechanism for the generated routes is proposed to manage the pool as follows.

First, for a generated route r_1, we ensure that it is not dominated by any routes in the pool. We examine whether it has the same customers as any other route in the pool. If such a route $r_2 \in \Omega$ exists and r_1 has a lower cost, then r_1 replaces r_2 in the pool. If such a route $r_2 \in \Omega$ exists but r_1 has a higher cost, we discard r_1.

Second, if a generated route r is unique and not dominated by the routes in Ω, we always add it to the pool if the pool's size does not exceed the limit ξ.

Third, if the size of the pool exceeds ξ, for a generated route r, we compute its reduced cost χ_r according to the Equation (53). If its reduced cost is negative, we add r into the Ω and remove the route with the highest reduced cost from Ω. If the reduced cost of r is non-negative, we will add it into a backup pool Ω_{back}.

Every n^{sp} iterations, an SP is formulated with the routes in Ω to obtain a new feasible solution S''. Then, an LP model of Ω is also formulated to update the dual value π_i of each customer i. Every n^{back} iterations, we compute the reduced cost for each route in Ω_{back}, and then add the routes with negative reduced costs to Ω, while removing the routes with the highest reduced cost from Ω.

Once the local optimal solution S' is obtained from the first component of our algorithm, we will try to add each feasible route r in S' into the pool Ω. Algorithm 5 presents the details of the route assembler.

6. Computational results

Section 6.1 describes the newly designed HEVRP-NL benchmark instances and the public E-VRP-NL benchmark instances from the literature. Section 6.2 provides details about the software and hardware used in our experiments. Section 6.3 presents the parameter settings for the proposed heuristic. Sections 6.4 to 6.7 present the computational results of HEVRP-NL instances. Sections 6.8 and 6.9 show the results of our heuristic when compared to state-of-the-art methods on E-VRP-NL and E-FSMFTW-PR benchmark instances, respectively.

Algorithm 5 The Route Assembler - $AssembelRoutes(S^{'}, \Omega, n)$

Parameters: n^{sp}, n^{back}
for each feasible route $r \in S^{'}$ **do**
  if r is unique in Ω and r is not dominated by other routes in Ω **then**
    if Ω is not full **then**
      Add the route r into Ω
    else if Ω is full **then**
      $\chi_r \leftarrow$ Compute the reduced cost of r
      if $\chi_r < 0$ **then**
        Using the filtering mechanism to add r into Ω
      else
        Add r into Ω_{back}
      end if
    end if
  end if
end for
if n mod $n^{back} \equiv 0$ **then**
  Using the filtering mechanism to choose the routes $r \in \Omega_{\text{back}}$ into Ω
end if
if n mod $n^{sp} \equiv 0$ **then**
  $S^{''} \leftarrow SetPartitioning(\Omega)$
  Update π_i by solve the LP model of the routes in Ω
end if
return $S^{''}$

6.1. Benchmark Instances

6.1.1. HEVRP-NL instances

We design the HEVRP-NL benchmark instances by extending the public E-FSMFTW instances of Hiermann et al. (2016). The E-FSMFTW instances only provide linear charging functions and do not consider congestion at CSs. Therefore, we need to design non-linear charging functions and time-dependent waiting functions for the CSs in each instance.

First, we introduce the E-FSMFTW instances. The instances are divided into three groups: A, B, and C, which correspond to the case of high, moderate, and low fixed EV costs, respectively. Each group is divided into six categories, based on their spatial (C, R, RC) and temporal (type-1, type-2) configurations. The customers in R instances are uniformly distributed, C instances contain clusters of customers, and RC instances are composed of some clusters and some uniformly distributed customers. In addition, the E-FSMFTW benchmark comprises a maximum of 6 EV types (ABCDEF) for each instance type. The RC2 instances comprise six EV types: ABCDEF. The R1 instances comprise five EV types: ABCDE. The R2, C2, and RC1 instances comprise four EV types: ABCD. The C1 instances comprise three EV types: ABC. There are 108 small-scale instances and 168 large-scale E-FSMFTW instances, which are used as HEVRP-NL benchmark instances. The sizes of small-scale instances are 5, 10, or 15 customers with 2 to 8 CSs. The size of large-scale instances is 100 customers

with 21 CSs. The parameter details are shown in Table 2.

Table 2: HEVRP-NL instance type parameters

Capacity/Electricity consumption modifier:							
Group	Inst.	A	B	C	D	E	F
ABC	R1	30/0.8	50/0.9	80/1.0	120/1.1	200/1.5	
	C1	100/0.9	200/1.0	300/1.1			
	RC1	40/0.85	80/0.95	150/1.05	200/1.15		
	R2	300/0.85	400/0.95	600/1.05	1000/1.15		
	C2	400/0.85	500/0.95	600/1.05	700/1.15		
	RC2	100/0.75	200/0.85	300/0.95	400/1.05	500/1.15	1000/1.25
Fixed Cost:							
Group	Inst.	A	B	C	D	E	F
A/B/C	R1	50/10/5	80/16/8	140/28/14	250/50/25	500/100/50	
	C1	300/60/30	800/160/80	1350/270/135			
	RC1	60/12/6	150/30/15	300/60/30	450/90/45		
	R2	450/90/45	700/140/70	1200/240/120	2500/500 /250		
	C2	1000/200 /100	1400/280 /140	2000/400/200	2700/540 /270		
	RC2	150/30/15	350/70/35	550/110/55	800/160/80	1100/220 /110	2500/500 /250

Second, we adopt the piecewise linear charging functions with multiple charging technologies (fast, normal, slow) of Montoya et al. (2017). We formulate three distinct charging rates and set two breakpoints at 0.95 and 0.85 of each EV type's maximum driving distance, which are consistent with Montoya et al. (2017). For each instance, the linear charging rate provided in E-FSMFTW is used as the basis for designing the non-linear charging function of normal CS. Then, we proportionally design the charging functions for fast CS and slow CS. Figure 4 illustrates the designed piecewise linear charging function of EV type k for the HEVRP-NL instances.

Third, we use the time-dependent waiting time functions in Keskin et al. (2019), which provided four waiting functions: TD-Steep-Long, TD-Steep-Short, TD-Smooth-Long, and TD-Smooth-Short, as shown in Fig 5. Steep and Smooth represent the types of transitions between off-peak time intervals and peak time intervals. Each transition type has two subtypes: one with long waiting times (Long) and the other with short waiting times (Short). The interval $[\alpha_0, \beta_0]$ is the time window of the depot. Similar to Keskin et al. (2019), we divide the day into four intervals (morning, noon, late afternoon, and evening) to simulate real-life waiting scenarios. The data of the depot opening time length in Keskin et al. (2019) is used as the basis for proportionally designing the waiting time functions for the HEVRP-NL instances.

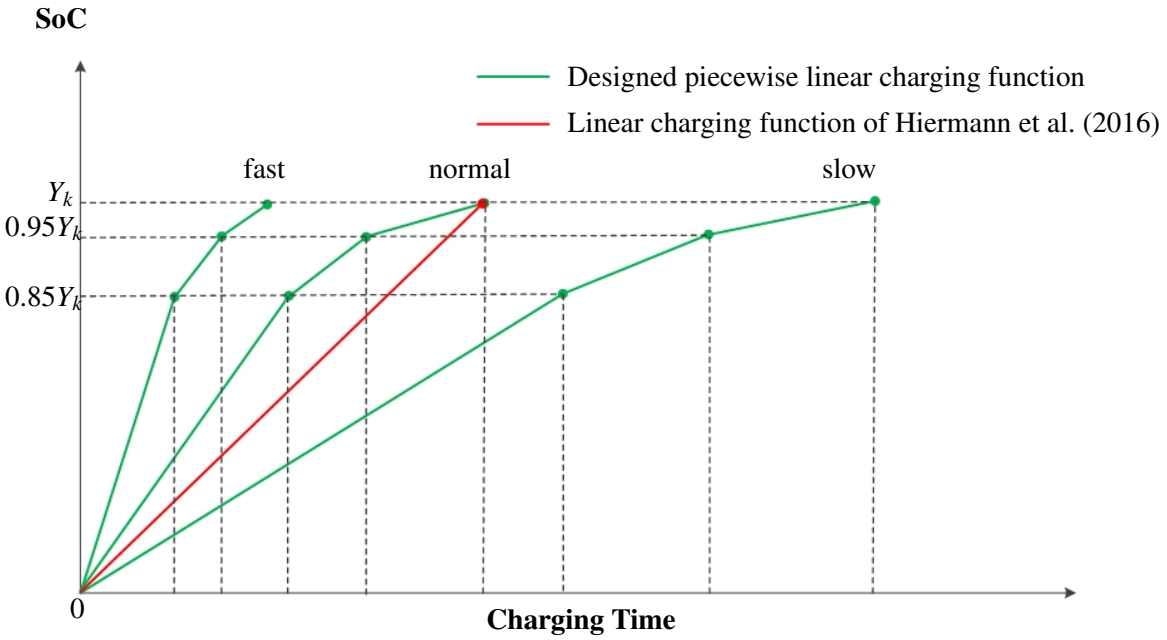

Figure 4: Designed piecewise linear charging function of EV type k for the HEVRP-NL instances

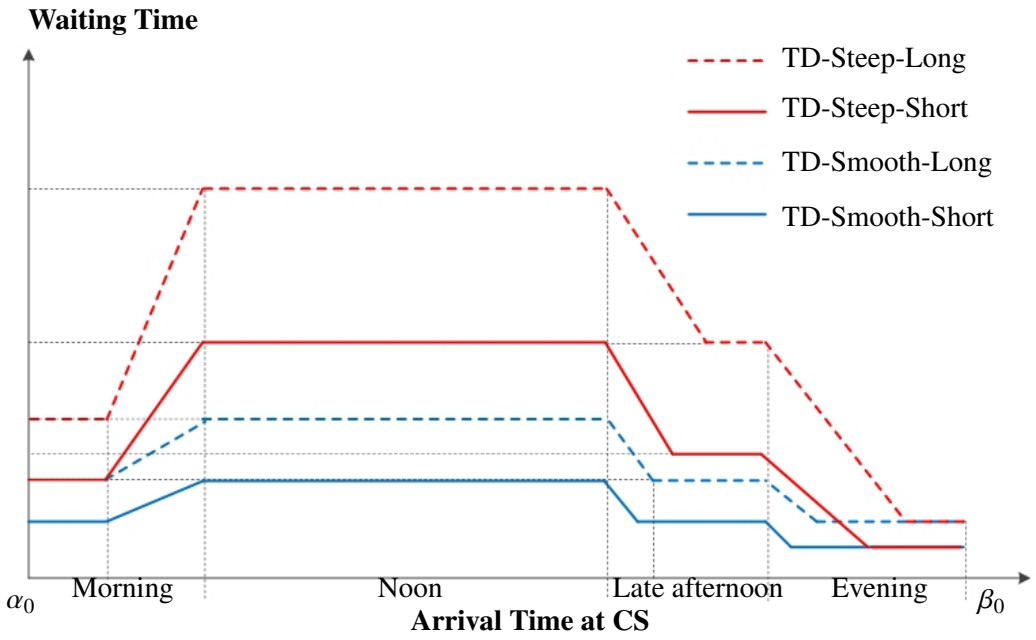

Figure 5: Designed time-dependent waiting functions at different CSs for the HEVRP-NL instances

Finally, the CSs in each HEVRP-NL instance are organized as follows. Regarding charging technologies, we arrange the CSs as fast CS, normal CS, and slow CS, in their order in the instances. Similarly, we arrange the waiting functions of CSs as TD-Smooth-Short, TD-Smooth-Long, TD-Steep-Short, and TD-Steep-Long, in their order in the instances.

6.1.2. E-VRP-NL instances

The E-VRP-NL benchmark instances were provided by Montoya et al. (2017). This benchmark includes a total of 120 instances. There are six sets of 20 instances, each with 10, 20, 40, 80, 160, or

320 customers. Each 10-customer instance contains 2 or 3 CSs. Each 20-customer instance contains 3 or 4 CSs. Each 40-customer instance contains 5 or 8 CSs. Each 80-customer instance contains 8 or 12 CSs. Each 160-customer instance contains 16 or 24 CSs. Each 320-customer instance contains 24 or 38 CSs. This benchmark provides a homogenous fleet of EVs and three piece-wise linear charging functions (fast, normal, and slow).

6.2. Software and hardware specifications

Our heuristic algorithm is implemented in Java, and the mathematical model is solved using IBM ILOG CPLEX 22.1.1.0. The experiments for the HEVRP-NL and the E-VRP-NL are conducted on a platform equipped with a 3.80-GHz AMD Core 3900x processor, 32 GB of RAM, and running Windows 10.

6.3. Parameter settings for the heuristic

The parameters of the heuristic algorithm are as follows: η_{penalty}, ε, λ_0, λ_{min}, λ_{max}, n_{sp}, n_{back}, ξ and n_{max}. The parameters η_{penalty}, ε, λ_0, λ_{min}, and λ_{max} are used for local search and are described in Section 5. The parameters n_{sp}, n_{back}, and ξ, described in Section 5.2.2, are used for managing the pool of a set partitioning model. The parameter n_{max} is the stopping criterion.

After some preliminary experiments on HEVRP-NL instances, we set the parameters of the heuristic as presented in Table 3.

Table 3: The paramters of the heuristic algorithm for the HEVRP-NL instances

η_{penalty}	ε	λ_0	λ_{min}	λ_{max}	n^{sp}	n^{back}	ξ	n^{max}
50	1.5	100	0.1	10000	1500	1500	5000	50000

6.4. Results for the small-scale HEVRP-NL instances

We use the proposed model and heuristic to solve 108 small-scale HEVRP-NL instances. The maximum running time for CPLEX is set to 3h. For each instance, our heuristic algorithm runs 10 times and we report the best result. The summary results are shown in Table 4, where “#Opt" represents the number of optimal solutions found, “#Num" represents the total number of instances, and “Avg Opt Gap" represents the average remaining optimal gap. In this table, “#Best" represents the number of best known solutions found by our heuristic algorithm, and “Best Gap" represents the gap between the best solution found by CPLEX and the best solution found by heuristic.

The summary results show that our model faces difficulties in solving 15-customer instances, can handle most of the 10-customer instances, and can solve all 5-customer instances. In the case of Group A instances, CPLEX obtains 23 optimal solutions, while for Group B and C instances, it achieves 25 optimal solutions for each group. In total, CPLEX finds 73 optimal solutions out of 108 instances.

Table 4: The summary results for small-scale HEVRP-NL instances

Group	N	CPLEX		Heuristic		
		#Opt/#Num	Avg Opt Gap	#Best	Avg Time (s)	Best Gap
A	5	12/12	0.00%			0.00%
	10	9/12	4.53%			-0.03%
	15	2/12	37.54%			-19.33%
	All	23/36	14.02%	36	1.92	-6.45%
B	5	12/12	0.00%			0.00%
	10	11/12	1.38%			0.00%
	15	2/12	28.49%			-15.19%
	All	25/36	9.96%	36	1.85	-5.06%
C	5	12/12	0.00%			0.00%
	10	11/12	0.54%			0.00%
	15	2/12	24.41%			-13.07%
	All	25/36	8.32%	36	1.70	-4.36%

Our heuristic algorithm is also capable of finding 73 optimal solutions which were determined by CPLEX in a very short time. For the remaining instances where CPLEX did not find the optimal solution, the heuristic finds high-quality local optimal solutions. Specifically, for the instances of Group A, Group B, and Group C, the heuristic algorithm provides solutions that are, on average, 6.45%, 5.06%, and 4.36% less costly than CPLEX. The detailed results for the small-scale HEVRP-NL instances are shown in Appendix B, which demonstrate the high performance of the heuristic.

6.5. Results for the large-scale HEVRP-NL instances

We conduct experiments on 168 large-scale HEVRP-NL instances, which are grouped into types A, B, and C. Each group contains 56 instances. We ran the heuristic algorithm 10 times for each instance, taking the best result as the Best Known Solution (BKS) for each instance. Table 5 presents a summary of the BKS for HEVRP-NL instances. “Cost" represents the average BKS value for each instance type. “Time" represents the average running time (minutes). “Fleet" shows the average number of each EV type used in the BKS. “NV" indicates the average number of EVs used in the BKS. “FC," “CC," and “TC" represent the proportions of fixed costs, charging time costs, and travel time costs to the total costs of BKS, respectively. The detailed results for the large-scale HEVRP-NL instances are shown in Appendix B.

The HEVRP-NL instances include up to six EV types labeled from A to F, where A is the smallest and F is the largest EV type. In the R1 instances, The BKS of R1 instances require 3 to 5 EV types, with a focus on middle-size types C and D. This suggests that scenarios with randomly distributed

customers and tight time windows require a combination of multiple EV types, particularly middle-size ones, to achieve high-quality solutions. The BKS of RC1 and RC2 instances require 3 to 4 EV types, primarily focusing on types B and C. The BKS of C1 instances only require two relatively small EV types, A and B. This is likely due to concentrated customer distributions and tight time windows, making it possible to achieve high-quality solutions with smaller vehicles. The BKS of C2 instances, with concentrated customer distributions and more lenient time windows, require only the smallest EV type A.

Table 5: The summary results of BKS for the large-scale HEVRP-NL instances (100 customers and 21 CSs)

Group	Instance	Cost	Time (min)	NV	Fleet	FC	CC	TC
A	C1	7520.56	13.81	19.00	$A^{19.00}$	75.79%	4.74%	19.46%
	C2	6588.85	17.53	5.63	$A^{5.63}$	85.37%	2.93%	11.70%
	R1	4177.63	16.54	20.17	$B^{4.58}C^{15.42}D^{0.17}$	61.44%	2.19%	36.37%
	R2	3152.58	12.79	5.00	$A^{5.00}$	71.37%	0.23%	28.40%
	RC1	5119.78	21.06	18.25	$A^{4.63}B^{6.63}C^{7.00}$	65.85%	1.81%	32.35%
	RC2	4204.28	22.51	11.63	$A^{5.88}B^{5.13}C^{0.63}$	71.80%	0.02%	28.18%
B	C1	2729.56	12.48	13.00	$A^{7.00}B^{6.00}$	50.56%	9.95%	39.50%
	C2	2101.42	22.26	5.75	$A^{5.75}$	54.72%	8.67%	36.61%
	R1	1987.65	13.60	14.75	$B^{1.00}C^{5.25}D^{7.83}E^{0.67}$	31.26%	4.27%	64.48%
	R2	1347.27	15.37	5.00	$A^{5.00}$	33.40%	0.56%	66.04%
	RC1	2304.75	12.76	14.50	$A^{0.63}B^{4.63}C^{7.75}D^{1.5}$	32.38%	3.90%	63.72%
	RC2	1687.40	11.82	7.38	$A^{1.13}B^{1.88}C^{4.38}$	38.30%	0.09%	61.61%
C	C1	2035.22	11.30	12.67	$A^{6.33}B^{6.33}$	34.23%	13.40%	52.37%
	C2	1524.91	23.12	5.63	$A^{4.88}B^{0.75}$	38.85%	11.75%	49.40%
	R1	1665.56	13.30	14.58	$A^{0.17}B^{1.25}C^{3.75}D^{8.25}E^{1.17}$	19.69%	4.86%	75.45%
	R2	1119.78	14.93	5.09	$A^{5.09}$	20.46%	0.49%	79.05%
	RC1	1914.88	12.51	14.13	$A^{0.50}B^{3.13}C^{7.88}D^{2.63}$	21.11%	4.15%	74.74%
	RC2	1361.22	11.73	7.00	$A^{1.00}B^{1.63}C^{3.75}D^{0.63}$	24.11%	0.18%	75.72%

FC: Fixed cost. CC: Charging time cost. TC: Travel time cost.

In terms of charging costs, The BKS of C1 instances have the highest proportion. This is because of tight time windows and low driving distance, necessitating frequent visits to CSs. The BKS of C2 and R2 instances have the next highest proportions. The BKS of R2 and RC2 instances have very low charging cost proportions (less than 1%), possibly due to their lenient time windows and driving distance, requiring almost no visits to CSs. Overall, the proportion of charging costs tends to increase from Group A to Group C instances. Travel time costs are highest in the R instances, followed by the RC instances, and are the lowest in the C instances. This aligns with intuition, as scenarios with randomly distributed customers require more time to serve customers, while cases with concentrated

customer distributions require less time.

6.6. Impact of non-linear charging functions for the large-scale HEVRP instances

In this section, we aim to investigate the benefits of incorporating non-linear charging functions, a key motivation in this study. Our approach involves the linearization of charging functions for each CS within the HEVRP instances while maintaining the original objective function. Subsequently, we applied our heuristic algorithm to each instance 10 times, selecting the best result as the BKS. We then conducted a detailed comparison of these outcomes with those derived from non-linear charging functions, as elaborated in Table 6. "NC-BKS" denotes the average BKS value considering the non-linear charging functions. "LC-BKS" represents the average BKS value considering the linear charging functions. Here, "Gap" represents the gap between "NC-BKS" and "LC-BKS".

Table 6: Comparison results of LC-BKS VS. NC-BKS for the large-scale HEVRP instances

Group	Instace	NC-BKS	LC-BKS	Gap	Instace	NC-BKS	LC-BKS	Gap
A	C1	7520.56	7656.35	-1.81%	C2	6588.85	6676.07	-1.32%
	R1	4177.63	4261.38	-2.00%	R2	3152.58	3154.50	-0.06%
	RC1	5119.78	5210.91	-1.78%	RC2	4204.28	4204.53	-0.01%
B	C1	2729.56	2866.55	-5.02%	C2	2101.42	2175.89	-3.54%
	R1	1987.65	2024.04	-1.83%	R2	1347.27	1349.57	-0.17%
	RC1	2304.75	2339.92	-1.53%	RC2	1687.40	1687.98	-0.03%
C	C1	2035.22	2149.98	-5.64%	C2	1524.91	1596.00	-4.66%
	R1	1665.56	1695.22	-1.78%	R2	1119.78	1121.87	-0.19%
	RC1	1914.88	1930.27	-0.80%	RC2	1361.22	1362.30	-0.08%

The results indicate that considering non-linear charging functions can significantly reduce costs for instances C1, C2, R1, and RC1. This suggests that for instances with tight time windows or concentrated customer distributions, incorporating non-linear charging (NC) functions can result in lower costs compared to linear charging (LC) functions. NC functions require less time for charging while potentially avoiding time window violations. For R2 and RC2 instances, the cost reduction from considering NC functions is also notable but relatively less significant. In summary, when considering NC functions, the average cost reduction for Group A, Group B, and Group C is on average 1.16%, 2.02%, and 2.19%, respectively.

We also report the total number of CSs visited in BKS of each instance type, which is shown in Table 7. Since the CSs have multiple charging technologies (fast, normal, slow), and we consider the charging time costs in objective function, it is expected that fast CSs have the highest frequency of visits, while slow CSs have the lowest.

Table 7: Number of CSs visited in each instance type

Charging Technologies	C1	C2	R1	R2	RC1	RC2	Total
Fast	213	109	319	59	177	2	879
Normal	79	31	236	19	163	10	538
Slow	0	3	50	12	34	1	100

6.7. Analysis of CS congestion on the large-scale HEVRP instances

We explore four levels of CS congestion, modeled as time-dependent waiting functions: TD-Smooth-Short, TD-Smooth-Long, TD-Steep-Short, and TD-Steep-Long. Based on the BKS results of large-scale HEVRP-NL instances, we conducted a statistical analysis of the frequency of EVs visiting CS for charging during different time intervals, which are shown in Table 8.

Table 8: Number of CSs visited during different time intervals

CS Congestion	Morning	Noon	Late Noon	Evening
TD-Smooth-Short	4	114	56	1
TD-Smooth-Long	142	147	223	10
TD-Steep-Short	31	205	59	0
TD-Steep-Long	201	107	214	3
Toal	378	573	552	14

The table shows that the majority of EVs tend to visit CSs during the noon and late noon time intervals, aligning with our intuition. This is because EVs depart from the depot fully charged in the morning, and by the evening, they are heading back to the depot without visiting any customers. However, we have also observed that the CSs with the shortest waiting times and least congestion (TD-Smooth-Short) are not the most frequently visited ones. This suggests that, when not considering waiting time costs, the charging technologies and geographic location of CSs have the most significant impact on routing costs, while the waiting time at CSs only needs to ensure compliance with time window constraints.

6.8. Computational comparisons on E-VRP-NL benchmark instances

The E-VRP-NL can be seen as a special case of the HEVRP-NL. To assess the performance of the proposed heuristic algorithm, we compared it with the state-of-the-art algorithms on the E-VRP-NL benchmark instances. Table 9 reports the summary results of the ILS with a heuristic concentration (ILS+HC) of Montoya et al. (2017), the large neighborhood search (LNS) of Koç et al. (2019), the ILS of Froger et al. (2022) and the ILS with a set partitioning model (ILS+SP) of our heuristic. “Best” represents the average value of the best solutions obtained by each algorithm. “Avg” represents the average value of the solutions obtained by each algorithm in 10 runs. “Time” is the average running time in seconds. The best values are indicated in bold.

Table 9: Comparison of the results obtained by the algorithms for the E-VRP-NL

N	ILS+HC			LNS			ILS			ILS+SP		
	Best	Avg	Time	Best	Avg	Time	Best	Avg	Time	Best	Avg	Time
10	**14.25**	14.31	5.65	**14.25**	14.27	8.25	**14.25**	**14.25**	4.60	**14.25**	**14.25**	**3.90**
20	19.44	19.52	10.50	19.43	19.47	14.35	**19.40**	**19.40**	8.40	**19.40**	**19.40**	**7.55**
40	31.48	31.99	35.45	31.49	31.56	45.45	**31.17**	31.18	20.00	**31.17**	**31.17**	**19.75**
80	38.01	38.79	80.10	38.04	38.27	99.30	36.61	36.83	**64.15**	**36.47**	**36.75**	77.90
160	70.24	71.38	568.05	70.51	71.17	631.85	65.41	66.01	**295.00**	**65.39**	**65.96**	378.05
320	132.47	134.97	4397.70	133.11	134.59	4555.15	118.66	119.33	**1117.65**	**118.54**	**119.32**	1472.55
CPU	Intel (2.33 GHz)			Intel (3.60 GHz)			Intel (3.06 GHz)			AMD (3.80 GHz)		

ILS+HC: Montoya et al. (2017), LNS: Koç et al. (2019), ILS: Froger et al. (2022).

The results presented in Table 9 demonstrate that our heuristic outperforms all existing methods in terms of solution quality. However, due to the multiple uses of the set partitioning model (SP) in our algorithm, as the problem size increases, the time required for solving SP also increases. This may lead to our algorithm having an average running time that appears to be higher than that of Froger et al. (2022) on 80-, 160- and 320-customer instances. Nevertheless, it is challenging to draw definitive conclusions about the time used by each algorithm since they were tested on different CPUs. The detailed results are reported in Appendix C.

Table 10: Comparison of the best solutions obtained by the algorithms for the E-VRP-NL

N	ILS+HC		LNS		ILS		ILS+SP			
	#BKS	Gap BKS	#BKS	Gap BKS	#BKS	Gap BKS	#Better	#Tie	#Worse	Gap BKS
10	20	0.00%	20	0.10%	20	0.00%	0	20	0	0.00%
20	11	0.30%	12	0.20%	20	0.00%	0	20	0	0.00%
40	3	1.00%	6	0.90%	20	0.00%	0	20	0	0.00%
80	0	3.80%	0	3.80%	20	0.00%	11	8	1	-0.35%
160	0	7.30%	0	7.70%	20	0.00%	7	7	6	-0.02%
320	0	11.20%	0	11.70%	20	0.00%	14	1	5	-0.11%
All		3.90%		4.10%		0.00%	32	76	12	-0.10%

ILS+HC: Montoya et al. (2017), LNS: Koç et al. (2019), ILS: Froger et al. (2022).

Finally, we report the best solutions found by each algorithm in Table 10. In this table, we define "BKS" as the best solutions found by algorithms in Montoya et al. (2017), Koç et al. (2019) and Froger et al. (2022) for each instance, "#BKS" denotes the number of BKS obtained, "Gap BKS" represents the average gap between the best solutions and the BKS for each algorithm, "#Better" is the number of solutions better than BKS, "#Tie" is the number of solutions same as BKS, and "#Worse" is the number of solutions worse than BKS.

Prior to this study, Froger et al. (2022) obtained the BKS for all instances. In this paper, our algorithm finds BKS for all 10-, 20-, and 40-customer instances. For the 80-, 160-, and 320-customer instances, we discovered 11 new best solutions, 7 new best solutions, and 14 new best solutions,

respectively. In total, we identify the best known solutions for 108 instances, 32 of which are new best solutions.

6.9. Computational comparisons on E-FSMFTW-PR benchmark instances

The E-FSMFTW-PR is a special case of HEVRP-NL when utilizing a partial charging policy, a linear charging function, and when waiting time is not allowed at CS. We compare the proposed heuristic with the state-of-the-art algorithm on 168 large-scale E-FSMFTW-PR instances. Table 11 reports the summary results of the hybrid heuristic (LNS+SP) of Wang & Zhao (2023), and our heuristic (ILS+SP). "Best 10" represents the average value of the best solutions obtained by each algorithm in 10 runs. "Time" is the average running time in minutes. "Gap" represents the average gap between these two algorithms.

Table 11: Comparison of the best solutions obtained by the algorithms for the large-scale E-FSMFTW-PR instances

Group	Instance	LNS+SP		ILS+SP		
		Best 10	Time (min)	Best 10	Time (min)	Gap (%)
A	C	6450.82	17.19	**6450.72**	**17.09**	0.00%
	R	3615.21	20.07	**3614.63**	**9.62**	-0.02%
	RC	4576.41	13.13	**4573.92**	**8.00**	-0.05%
B	C	2079.87	22.34	**2079.35**	**9.99**	-0.02%
	R	1608.84	24.10	**1605.67**	**9.28**	-0.20%
	RC	1910.60	18.64	**1905.81**	**8.65**	-0.25%
C	C	1476.27	19.79	**1476.27**	**9.89**	0.00%
	R	1331.89	21.05	**1330.69**	**9.10**	-0.09%
	RC	1553.17	14.58	**1552.27**	**8.30**	-0.06%

LNS+SP: Wang & Zhao (2023)

It can be observed from the table that our algorithm outperforms the algorithm of Wang & Zhao (2023) in both solution quality and solution time. In total, we identify the best-known solutions for 163 instances, 33 of which are new best solutions. The detailed comparison results of the best-known solutions (BKS) are reported in Appendix D.

7. Conclusion

This paper introduces a Heterogeneous-Fleet Electric Vehicle Routing Problem that incorporates nonlinear charging and waiting time functions, which represents a very realistic scenario in practice. First, we formulate a MILP model capable of solving small-scale instances to optimality or providing good feasible solutions. Subsequently, we propose a hybrid heuristic algorithm that comprises two critical components: a route evaluation function for efficient cost computation of a fixed route, and a pool for storing feasible routes which are assembled into a new solution by using a set-partitioning model. The heuristic algorithm finds optimal solutions for small-scale instances rapidly, while for

large-scale instances, we provide detailed information on local optimal solutions. We analyze the fleet composition and demonstrate the benefits of considering non-linear charging functions. To assess the performance of our algorithm, we conducted experiments on 120 public E-VRP-NL instances and 168 public E-FSMFTW-PR instances. Our algorithm finds 32 new best solutions for E-VRP-NL and 33 new best solutions for E-FSMFTW-PR, respectively.

Funding

This research was supported by the Chinese Fundamental Research Funds for the Central Universities in UIBE (22YB01).

Data Availability

The E-FSMFTW benchmark instances are available for download at https://data.mendeley.com/datasets/h3mrm5dhxw/1. The E-VRP-NL benchmark instances are available for download at http://vrp-rep.org.

Declaration of Competing Interest

No potential conflict of interest was reported by the author(s).

References

Andelmin, J., & Bartolini, E. (2017). An exact algorithm for the green vehicle routing problem. *Transportation Science*, *51*, 1288–1303.

Basso, R., Kulcsár, B., & Sanchez-Diaz, I. (2021). Electric vehicle routing problem with machine learning for energy prediction. *Transportation Research Part B: Methodological*, *145*, 24–55.

Bruglieri, M., Mancini, S., Pezzella, F., & Pisacane, O. (2019a). A path-based solution approach for the green vehicle routing problem. *Computers & Operations Research*, *103*, 109–122.

Bruglieri, M., Mancini, S., & Pisacane, O. (2019b). The green vehicle routing problem with capacitated alternative fuel stations. *Computers & Operations Research*, *112*, 104759.

Bruglieri, M., Paolucci, M., & Pisacane, O. (2023). A matheuristic for the electric vehicle routing problem with time windows and a realistic energy consumption model. *Computers & Operations Research*, *157*, 106261.

Çatay, B., & Sadati, İ. (2023). An improved matheuristic for solving the electric vehicle routing problem with time windows and synchronized mobile charging/battery swapping. *Computers & Operations Research*, *159*, 106310.

Cortés-Murcia, D. L., Prodhon, C., & Afsar, H. M. (2019). The electric vehicle routing problem with time windows, partial recharges and satellite customers. *Transportation Research Part E: Logistics and Transportation Review*, *130*, 184–206.

Desaulniers, G., Errico, F., Irnich, S., & Schneider, M. (2016). Exact algorithms for electric vehicle-routing problems with time windows. *Operations Research*, *64*, 1388–1405.

Desaulniers, G., Gschwind, T., & Irnich, S. (2020). Variable fixing for two-arc sequences in branch-price-and-cut algorithms on path-based models. *Transportation Science*, *54*, 1170–1188.

Erdoğan, S., & Miller-Hooks, E. (2012). A green vehicle routing problem. *Transportation Research Part E: Logistics and Transportation Review*, *48*, 100–114.

Felipe, Á., Ortuño, M. T., Righini, G., & Tirado, G. (2014). A heuristic approach for the green vehicle routing problem with multiple technologies and partial recharges. *Transportation Research Part E: Logistics and Transportation Review*, *71*, 111–128.

Froger, A., Jabali, O., Mendoza, J. E., & Laporte, G. (2022). The electric vehicle routing problem with capacitated charging stations. *Transportation Science*, *56*, 460–482.

Froger, A., Mendoza, J. E., Jabali, O., & Laporte, G. (2019). Improved formulations and algorithmic components for the electric vehicle routing problem with nonlinear charging functions. *Computers & Operations Research*, *104*, 256–294.

Gnann, T., Funke, S., Jakobsson, N., Plötz, P., Sprei, F., & Bennehag, A. (2018). Fast charging infrastructure for electric vehicles: Today's situation and future needs. *Transportation Research Part D: Transport and Environment*, *62*, 314–329.

Goeke, D., & Schneider, M. (2015). Routing a mixed fleet of electric and conventional vehicles. *European Journal of Operational Research*, *245*, 81–99.

Hiermann, G., Hartl, R. F., Puchinger, J., & Vidal, T. (2019). Routing a mix of conventional, plug-in hybrid, and electric vehicles. *European Journal of Operational Research*, *272*, 235–248.

Hiermann, G., Puchinger, J., Ropke, S., & Hartl, R. F. (2016). The electric fleet size and mix vehicle routing problem with time windows and recharging stations. *European Journal of Operational Research*, *252*, 995–1018.

Hof, J., Schneider, M., & Goeke, D. (2017). Solving the battery swap station location-routing problem with capacitated electric vehicles using an avns algorithm for vehicle-routing problems with intermediate stops. *Transportation Research Part B: Methodological*, *97*, 102–112.

Jie, W., Yang, J., Zhang, M., & Huang, Y. (2019). The two-echelon capacitated electric vehicle routing problem with battery swapping stations: Formulation and efficient methodology. *European Journal of Operational Research*, *272*, 879–904.

Keskin, M., & Çatay, B. (2016). Partial recharge strategies for the electric vehicle routing problem with time windows. *Transportation Research Part C: Emerging Technologies*, *65*, 111–127.

Keskin, M., & Çatay, B. (2018). A matheuristic method for the electric vehicle routing problem with time windows and fast chargers. *Computers & Operations Research*, *100*, 172–188.

Keskin, M., Çatay, B., & Laporte, G. (2021). A simulation-based heuristic for the electric vehicle routing problem with time windows and stochastic waiting times at recharging stations. *Computers & Operations Research*, *125*, 105060.

Keskin, M., Laporte, G., & Çatay, B. (2019). Electric vehicle routing problem with time-dependent waiting times at recharging stations. *Computers & Operations Research*, *107*, 77–94.

Koç, Ç., Jabali, O., Mendoza, J. E., & Laporte, G. (2019). The electric vehicle routing problem with shared charging stations. *International Transactions in Operational Research*, *26*, 1211–1243.

Kullman, N. D., Goodson, J. C., & Mendoza, J. E. (2021). Electric vehicle routing with public charging stations. *Transportation Science*, *55*, 637–659.

Lam, E., Desaulniers, G., & Stuckey, P. J. (2022). Branch-and-cut-and-price for the electric vehicle routing problem with time windows, piecewise-linear recharging and capacitated recharging stations. *Computers & Operations Research*, *145*, 105870.

Lee, C. (2021). An exact algorithm for the electric-vehicle routing problem with nonlinear charging time. *Journal of the Operational Research Society*, *72*, 1461–1485.

Lera-Romero, G., Bront, J. J. M., & Soulignac, F. J. (2024). A branch-cut-and-price algorithm for the time-dependent electric vehicle routing problem with time windows. *European Journal of Operational Research*, *312*, 978–995.

Macrina, G., Laporte, G., Guerriero, F., & Pugliese, L. D. P. (2019). An energy-efficient green-vehicle routing problem with mixed vehicle fleet, partial battery recharging and time windows. *European Journal of Operational Research*, *276*, 971–982.

Montoya, A., Guéret, C., Mendoza, J. E., & Villegas, J. G. (2017). The electric vehicle routing problem with nonlinear charging function. *Transportation Research Part B: Methodological*, *103*, 87–110.

Pelletier, S., Jabali, O., & Laporte, G. (2018). Charge scheduling for electric freight vehicles. *Transportation Research Part B: Methodological*, *115*, 246–269.

Pelletier, S., Jabali, O., & Laporte, G. (2019). The electric vehicle routing problem with energy consumption uncertainty. *Transportation Research Part B: Methodological*, *126*, 225–255.

Pelletier, S., Jabali, O., Laporte, G., & Veneroni, M. (2017). Battery degradation and behaviour for electric vehicles: Review and numerical analyses of several models. *Transportation Research Part B: Methodological*, *103*, 158–187.

Raeesi, R., & Zografos, K. G. (2020). The electric vehicle routing problem with time windows and synchronised mobile battery swapping. *Transportation Research Part B: Methodological*, *140*, 101–129.

Roberti, R., & Wen, M. (2016). The electric traveling salesman problem with time windows. *Transportation Research Part E: Logistics and Transportation Review*, *89*, 32–52.

Schiffer, M., & Walther, G. (2017). The electric location routing problem with time windows and partial recharging. *European Journal of Operational Research*, *260*, 995–1013.

Schiffer, M., & Walther, G. (2018). An adaptive large neighborhood search for the location-routing problem with intra-route facilities. *Transportation Science*, *52*, 331–352.

Schneider, M., Stenger, A., & Goeke, D. (2014). The electric vehicle-routing problem with time windows and recharging stations. *Transportation Science*, *48*, 500–520.

Uhrig, M., Weiß, L., Suriyah, M., & Leibfried, T. (2015). E-mobility in car parks–guidelines for charging infrastructure expansion planning and operation based on stochastic simulations. In *EVS28 International Electric Vehicle Symposium and Exhibition* (pp. 1–12).

Vidal, T., Crainic, T. G., Gendreau, M., & Prins, C. (2013). A hybrid genetic algorithm with adaptive diversity management for a large class of vehicle routing problems with time-windows. *Computers & Operations Research*, *40*, 475–489.

Wang, W., & Zhao, J. (2023). Partial linear recharging strategy for the electric fleet size and mix vehicle routing problem with time windows and recharging stations. *European Journal of Operational Research*, *308*, 929–948.

Zhang, S., Gajpal, Y., Appadoo, S., & Abdulkader, M. (2018). Electric vehicle routing problem with recharging stations for minimizing energy consumption. *International Journal of Production Economics*, *203*, 404–413.

Zhou, Y., Meng, Q., & Ong, G. P. (2022). Electric bus charging scheduling for a single public transport route considering nonlinear charging profile and battery degradation effect. *Transportation Research Part B: Methodological*, *159*, 49–75.

Appendix A. Algorithmic details for the Route Evaluation

Algorithm 6 illustrates the methodology for determining the current maximum available charging time at a CS node. Algorithm 7 outlines the procedure for calculating the maximum allowable delay time at a CS node. Algorithm 8 details the process of obtaining the maximum shift time at a CS node, which can be used for charging or waiting. Algorithm 9 provides a detailed description to perform the charging time at a CS node.

Appendix B. Detailed results for the HEVRP-NL instances

The detailed results for the small-scale HEVRP-NL instances are shown in Tables B1, B2 and B3. “UB" represents the optimal solution or upper-bound solution found by CPLEX. “LB" represents the lower-bound solution of CPLEX. “Δ_{opt}” represents the remaining optimality gap of CPLEX. “Cost" represents the best solution found by heuristic. “Gap" represents the gap between “UB" and “Cost".

The detailed results for the large-scale HEVRP-NL instances are shown in Tables B4, B5, and B6. For each instance, our heuristic algorithm will run 10 times. “Avg 10”, “Best 10” and “Time” represent the average result, the best result, and the average running time, respectively.

Appendix C. Detailed comparison results for the E-VRP-NL instances

E-VRP-NL Instances are labeled according to the convention tcAcBsCcDE, where:

A represents the method used for customer placement (0: random uniform, 1: clustered, 2: mixture of both), B indicates the number of customers, C represents the number of charging stations (CSs), D is ’t’ if the CSs are located using a p-median heuristic and ’f’ if the CSs were randomly located, E signifies the instance number for each combination of parameters (i.e., E=0,1,2,3,4).

The detailed comparison results for 120 E-VRP-NL benchmark instances are shown in Tables C1 and C2. These two tables report the detailed results obtained by our heuristic (ILS+SP), the ILS with a heuristic concentration (ILS+HC) of Montoya et al. (2017), the large neighborhood search (LNS) of Koç et al. (2019), and the ILS of Froger et al. (2022).

"Best" and "Avg" represent the values of the best solutions and the average values of solutions obtained by an algorithm in 10 runs. "T" is the average running time in seconds. For each instance, "Best Gap" represents the gap between the best-known solution prior to this paper and the best solution obtained by our heuristic. For the column "Best" of our algorithm, the values of the best solutions are indicated in boldface, and the values of the new best solutions are underlined.

Appendix D. Detailed comparison results for the large-scale E-FSMFTW-PR instances

The detailed results for the large-scale E-FSMFTW-PR instances are shown in Table D1. For each instance, our heuristic algorithm will run 10 times. "LNS+SP" represents the best results of Wang & Zhao (2023). "ILS+SP" represents the best results of our proposed algorithm. "Time" represents the average running time in minutes. The values of the best solutions are indicated in boldface, and the values of the new best solutions are underlined.

Algorithm 6 *Get_Max_Charging_Time*(c, q)

Input: CS node c, the maximum chargeable amount of SoC q, q_c^{lea} is within the piecewise linear SoC interval of $\left[\underline{q}, \overline{q}\right]$ and the corresponding charging slope is ρ
Output: the maximum charging time T_c^{charge} at CS node c
$T_c^{charge} \leftarrow Min(q, (\overline{q} - q_c^{lea}))/\rho$
$T^{temp} \leftarrow T_c^{charge}$
for $i \in \{CS_c, \ldots, CS_n, 0\}$ **do**
    $T_i^{shift} \leftarrow Get\_Max\_Shift\_Time(i)$ ..... (see Algorithm 8)
    if $T^{temp} > T_i^{shift}$ **then**
        $T_c^{charge} \leftarrow T_c^{charge} - (T^{temp} - T_i^{shift})$
        $T^{temp} \leftarrow Max(0, T_i^{shift} - T_i^{slack})$
    else
        $T^{temp} \leftarrow Max(0, T^{temp} - T_i^{slack})$
    end if
    if $T^{temp} = 0$ **then**
        break
    end if
end for
return T_c^{charge}

Algorithm 7 *Get_Max_Delay_Time*(c)

Input: CS node c
Output: the maximum delay time T^{delay} at CS node c
$T^{delay} \leftarrow Get\_Max\_Shift\_Time(c)$ ..... (see Algorithm 8)
$T^{temp} \leftarrow T^{delay}$
for $i \in \{CS_c, \ldots, CS_n, 0\}$ **do**
    $T_i^{shift} \leftarrow Get\_Max\_Shift\_Time(i)$ ..... (see Algorithm 8)
    if $T^{temp} > T_i^{shift}$ **then**
        $T^{delay} \leftarrow T^{delay} - (T^{temp} - T_i^{shift})$
        $T^{temp} \leftarrow Max(0, T_i^{shift} - T_i^{slack})$
    else
        $T^{temp} \leftarrow Max(0, T^{temp} - T_i^{slack})$
    end if
    if $T^{temp} = 0$ **then**
        break
    end if
end for
return T^{delay}

Algorithm 8 $Get\_Max\_Shift\_Time(c)$

Input: the time intervals $\mathcal{M}_c$ of the $W_c(t)$ function at CS c, the m^{th} arrival time interval $\left[\underline{a_m}, \overline{a_m}\right]$ and the corresponding waiting slope is ρ_m, T_i^{max}, T_i^{arr}, T_i^W
Output: the maximum shift time T_i^{shift} at CS node c
$T_i^{shift} \leftarrow 0$, $T^{max} \leftarrow T_i^{max}$, $T^W \leftarrow T_i^W$, $T^{arr} \leftarrow T_i^{arr}$
for $m \in \{0, \ldots, \mathcal{M}_c\}$ **do**
  if $\underline{a_m} \leq T^{arr} \leq \overline{a_m}$ **then**
    $T^{rest} \leftarrow \overline{a_m} - T^{arr}$
    $T^{newwait} \leftarrow T^W + \rho_m * T^{rest}$
    if $T^{newwait} + T^{rest} \leq T^{max}$ **then**
      $T^{max} \leftarrow T^{max} - T^{rest}$
      $T^W \leftarrow T^{newwait}$
      $T^{arr} \leftarrow \overline{a_m}$
      $T_i^{shift} \leftarrow T_i^{shift} + T^{rest}$
    else
      $T^{temp} \leftarrow (T^{max} - T^W)/(1 + \rho_m)$
      if $T^{temp} \leq 0$ **then**
        return 0
      end if
      $T_i^{shift} \leftarrow T_i^{shift} + T^{temp}$
      return T_i^{shift}
    end if
  end if
end for

Algorithm 9 $PeformChargeTime(c, T^{charge})$

$\rho \leftarrow$ the current charging slope at CS c
for $i \in \{CS_{c+1}, \ldots, CS_n, 0\}$ **do**
  $q_i^{arr} \leftarrow q_i^{arr} + \rho * T^{charge}$
  $q_i^{lea} \leftarrow q_i^{lea} + \rho * T^{charge}$
end for
for $i \in \{CS_c, \ldots, CS_n, 0\}$ **do**
  if $i \neq CS_c$ **then**
    $T_i^{arr} \leftarrow T_i^{arr} + T^{charge}$
  end if
  $T_i^{max} \leftarrow T_i^{max} - T^{charge}$,
  $T^{temp} \leftarrow T^{charge}$, $T^{charge} \leftarrow Max(0, T^{charge} - T_i^{slack})$
  $T_i^{slack} \leftarrow Max(0, T_i^{slack} - T^{temp})$
  if $T^{charge} = 0$ **then**
    break
  end if
end for
for $i \in \{CS_c, \ldots, CS_n\}$ **do**
  $T_i^W \leftarrow W_i(T_i^{arr})$
end for

Table B1: Detailed results for the small-scale HEVRP-NL instances of Group A

Instance	CPLEX				Heuristic		
	UB	LB	Δ_{opt}	Time (s)	Cost	Time (s)	Gap
C101-5	1158.68	–	0.00%	0.41	1158.68	0.45	0.00%
C103-5	644.60	–	0.00%	1.41	644.60	0.44	0.00%
C206-5	2108.06	–	0.00%	8.59	2108.06	0.67	0.00%
C208-5	1528.38	–	0.00%	1.98	1528.38	0.31	0.00%
R104-5	338.58	–	0.00%	6.30	338.58	0.35	0.00%
R105-5	363.85	–	0.00%	0.39	363.85	0.38	0.00%
R202-5	643.85	–	0.00%	10.77	643.85	0.53	0.00%
R203-5	692.27	–	0.00%	10.17	692.27	0.79	0.00%
RC105-5	524.49	–	0.00%	0.39	524.49	0.48	0.00%
RC108-5	648.05	–	0.00%	4.33	648.05	0.41	0.00%
RC204-5	514.12	–	0.00%	12.91	514.12	0.69	0.00%
RC208-5	385.74	–	0.00%	11.53	385.74	0.66	0.00%
C101-10	1769.04	–	0.00%	5.00	1769.04	1.18	0.00%
C104-10	1276.97	1197.44	6.23%	10800	1272.33	1.13	-0.36%
C202-10	1759.69	–	0.00%	86.31	1759.69	1.98	0.00%
C205-10	2967.77	–	0.00%	270.20	2967.77	1.03	0.00%
R102-10	628.69	–	0.00%	544.80	628.69	0.72	0.00%
R103-10	495.60	–	0.00%	5244.55	495.60	0.79	0.00%
R201-10	1196.28	–	0.00%	151.50	1196.28	1.61	0.00%
R203-10	1034.19	757.84	26.72%	10800	1034.19	1.38	0.00%
RC102-10	1134.92	–	0.00%	7.76	1134.92	0.85	0.00%
RC108-10	763.22	–	0.00%	5317.58	763.22	0.91	0.00%
RC201-10	753.18	–	0.00%	38.55	752.20	1.78	-0.13%
RC205-10	1113.32	875.42	21.37%	10800	1113.32	1.76	0.00%
C103-15	1825.18	1360.77	25.44%	10800	1684.63	2.66	-7.70%
C106-15	1640.55	–	0.00%	526.67	1640.55	2.52	0.00%
C202-15	6399.68	1570.13	75.47%	10800	4003.95	2.57	-37.44%
C208-15	2987.92	1845.83	38.22%	10800	2987.92	3.86	0.00%
R102-15	950.45	825.78	13.12%	10800	950.45	3.86	0.00%
R105-15	806.78	–	0.00%	520.80	806.78	2.83	0.00%
R202-15	5267.87	781.51	85.16%	10800	1855.00	6.11	-64.79%
R209-15	3812.99	688.67	81.94%	10800	1569.44	6.72	-58.84%
RC103-15	886.50	781.91	11.80%	10800	884.56	2.42	-0.22%
RC108-15	1156.62	910.63	21.27%	10800	1091.44	2.01	-5.64%
RC202-15	1659.11	787.80	52.52%	10800	1358.46	4.86	-18.12%
RC204-15	1434.37	780.82	45.56%	10800	871.71	7.46	-39.23%

Table B2: Detailed results for the small-scale HEVRP-NL instances of Group B

Instance	CPLEX				Heuristic		
	UB	LB	Δ_{opt}	Time (s)	Cost	Time (s)	Gap
C101-5	566.40	–	0.00%	0.33	566.40	0.48	0.00%
C103-5	323.23	–	0.00%	0.39	323.23	0.41	0.00%
C206-5	917.70	–	0.00%	8.22	917.70	0.69	0.00%
C208-5	728.38	–	0.00%	5.11	728.38	0.31	0.00%
R104-5	186.58	–	0.00%	3.05	186.58	0.34	0.00%
R105-5	211.85	–	0.00%	0.31	211.85	0.4	0.00%
R202-5	283.85	–	0.00%	10.56	283.85	0.54	0.00%
R203-5	332.27	–	0.00%	9.05	332.27	0.68	0.00%
RC105-5	308.49	–	0.00%	0.38	308.49	0.45	0.00%
RC108-5	396.65	–	0.00%	3.91	396.65	0.37	0.00%
RC204-5	274.12	–	0.00%	21.64	274.12	0.63	0.00%
RC208-5	265.74	–	0.00%	21.91	265.74	0.83	0.00%
C101-10	990.91	–	0.00%	6.81	990.91	1.49	0.00%
C104-10	760.59	–	0.00%	10311.05	760.59	1.72	0.00%
C202-10	948.51	–	0.00%	605.56	948.51	1.63	0.00%
C205-10	1047.77	–	0.00%	35.70	1047.77	1.21	0.00%
R102-10	348.69	–	0.00%	42.25	348.69	0.95	0.00%
R103-10	279.60	–	0.00%	7206.00	279.60	1.12	0.00%
R201-10	476.28	–	0.00%	119.83	476.28	2.51	0.00%
R203-10	448.87	374.45	16.58%	10800	448.87	2.55	0.00%
RC102-10	606.92	–	0.00%	11.17	606.92	1.24	0.00%
RC108-10	475.22	–	0.00%	463.00	475.22	1.34	0.00%
RC201-10	491.03	–	0.00%	33.17	491.03	2.37	0.00%
RC205-10	553.32	–	0.00%	1958.94	553.32	2.51	0.00%
C103-15	861.62	769.97	10.64%	10800	861.62	2.01	0.00%
C106-15	828.75	–	0.00%	60.69	828.75	1.51	0.00%
C202-15	2074.92	991.17	52.23%	10800	1547.55	3.41	-25.42%
C208-15	1376.56	1033.46	24.92%	10800	1330.95	2.14	-3.31%
R102-15	594.82	561.68	5.57%	10800	594.82	2.62	0.00%
R105-15	479.25	–	0.00%	222.72	479.25	2.04	0.00%
R202-15	1397.14	480.65	65.60%	10800	784.61	5.69	-43.84%
R209-15	1369.69	402.41	70.62%	10800	649.44	7.29	-52.59%
RC103-15	530.63	503.23	5.16%	10800	530.63	2.05	0.00%
RC108-15	580.62	488.35	15.89%	10800	580.62	1.63	0.00%
RC202-15	728.77	518.06	28.91%	10800	707.82	5.37	-2.87%
RC204-15	1021.18	384.67	62.33%	10800	467.65	4.11	-54.21%

Table B3: Detailed results for the small-scale HEVRP-NL instances of Group C

Instance	CPLEX				Heuristic		
	UB	LB	Δ_{opt}	Time (s)	Cost	Time (s)	Gap
C101-5	467.91	–	0.00%	0.33	467.91	0.49	0.00%
C103-5	263.23	–	0.00%	0.42	263.23	0.39	0.00%
C206-5	716.50	–	0.00%	9.16	716.50	0.54	0.00%
C208-5	609.85	–	0.00%	6.38	609.85	0.34	0.00%
R104-5	167.58	–	0.00%	2.25	167.58	0.36	0.00%
R105-5	192.85	–	0.00%	0.33	192.85	0.38	0.00%
R202-5	238.85	–	0.00%	10.19	238.85	0.53	0.00%
R203-5	287.27	–	0.00%	7.80	287.27	0.64	0.00%
RC105-5	281.49	–	0.00%	0.42	281.49	0.43	0.00%
RC108-5	336.65	–	0.00%	4.00	336.65	0.41	0.00%
RC204-5	244.12	–	0.00%	24.13	244.12	0.54	0.00%
RC208-5	250.74	–	0.00%	26.25	250.74	0.54	0.00%
C101-10	840.91	–	0.00%	8.78	840.91	1.64	0.00%
C104-10	621.02	–	0.00%	2031.41	621.02	1.22	0.00%
C202-10	748.37	–	0.00%	705.81	748.37	1.48	0.00%
C205-10	806.09	–	0.00%	19.64	806.09	0.95	0.00%
R102-10	313.69	–	0.00%	31.38	313.69	1.04	0.00%
R103-10	249.81	233.82	6.40%	10800	249.81	1.08	0.00%
R201-10	386.28	–	0.00%	133.03	386.28	2.26	0.00%
R203-10	378.34	–	0.00%	10656.06	378.34	3.16	0.00%
RC102-10	540.56	–	0.00%	6.45	540.56	1.26	0.00%
RC108-10	439.22	–	0.00%	543.73	439.22	1.16	0.00%
RC201-10	436.85	–	0.00%	62.56	436.85	1.99	0.00%
RC205-10	483.32	–	0.00%	844.84	483.32	2.21	0.00%
C103-15	741.62	684.87	7.65%	10800	741.62	1.95	0.00%
C106-15	678.75	–	0.00%	470.03	678.75	1.51	0.00%
C202-15	1354.35	898.08	33.69%	10800	1184.43	2.97	-12.55%
C208-15	1071.96	851.02	20.61%	10800	1016.76	2.16	-5.15%
R102-15	533.47	508.67	4.65%	10800	533.47	2.26	0.00%
R105-15	430.25	–	0.00%	40.47	430.25	1.87	0.00%
R202-15	1234.34	430.49	65.12%	10800	649.24	5.76	-47.40%
R209-15	927.91	355.92	61.64%	10800	534.41	4.99	-42.41%
RC103-15	479.63	457.01	4.72%	10800	479.63	2.29	0.00%
RC108-15	508.62	428.50	15.75%	10800	508.62	1.59	0.00%
RC202-15	656.75	473.09	27.97%	10800	592.31	4.69	-9.81%
RC204-15	691.01	337.50	51.16%	10800	417.65	4.15	-39.56%

Table B4: Detailed results for the large-scale HEVRP-NL instances of Group A (100 customers and 21 CSs)

Instance	Avg 10	Best 10	Time (min)	Instance	Avg 10	Best 10	Time (min)
C101	7563.73	7552.46	13.64	R201	3453.39	3436.27	19.89
C102	7519.84	7517.74	11.83	R202	3294.12	3266.96	15.96
C103	7519.19	7508.28	13.64	R203	3171.46	3137.78	12.53
C104	7487.80	7476.00	13.46	R204	3012.95	3007.93	8.48
C105	7554.46	7547.23	11.12	R205	3279.31	3259.05	15.41
C106	7554.90	7543.88	14.47	R206	3197.73	3173.24	14.31
C107	7540.01	7537.97	14.71	R207	3120.56	3079.41	9.56
C108	7529.81	7518.01	15.77	R208	3008.75	2996.15	10.12
C109	7495.28	7483.44	15.67	R209	3173.94	3150.90	14.83
C201	7009.37	6972.00	17.68	R210	3145.03	3128.62	11.43
C202	6997.06	6969.87	15.31	R211	3065.42	3042.10	10.21
C203	6953.61	6945.76	16.25	RC101	5510.76	5428.90	24.14
C204	5981.87	5976.95	18.06	RC102	5307.93	5271.71	22.36
C205	6957.16	6946.43	19.81	RC103	5187.91	5066.96	19.36
C206	6046.60	6033.21	21.05	RC104	4964.80	4899.06	20.11
C207	6965.93	6926.88	14.71	RC105	5293.55	5249.05	21.16
C208	5978.59	5939.74	17.33	RC106	5182.91	5093.75	22.15
R101	4578.31	4545.94	17.14	RC107	5023.67	4999.00	20.25
R102	4379.10	4353.04	16.41	RC108	5078.33	4949.81	18.96
R103	4212.40	4190.24	18.33	RC201	4392.84	4337.60	24.24
R104	4093.72	4085.60	16.20	RC202	4301.79	4261.89	24.08
R105	4304.99	4283.87	18.43	RC203	4201.06	4147.68	24.72
R106	4211.95	4192.88	16.90	RC204	4196.91	4107.84	18.16
R107	4131.21	4106.38	18.01	RC205	4353.32	4254.70	23.94
R108	4091.55	4062.28	17.05	RC206	4252.53	4237.42	26.14
R109	4148.20	4122.12	17.15	RC207	4275.85	4181.92	18.06
R110	4093.20	4070.78	16.04	RC208	4156.17	4105.21	20.72
R111	4196.45	4069.45	12.32				
R112	4064.08	4048.95	14.46				

Table B5: Detailed results for the large-scale HEVRP-NL instances of Group B (100 customers and 21 CSs)

Instance	Avg 10	Best 10	Time (min)	Instance	Avg 10	Best 10	Time (min)
C101	2873.71	2812.79	12.88	R201	1656.81	1628.76	24.72
C102	2800.46	2728.82	12.16	R202	1482.30	1473.24	15.69
C103	2767.06	2727.58	12.81	R203	1354.73	1337.64	14.68
C104	2659.14	2570.26	12.24	R204	1234.59	1207.03	10.14
C105	2877.10	2772.03	12.26	R205	1479.85	1451.64	19.90
C106	2802.08	2764.59	12.73	R206	1396.23	1374.71	19.21
C107	2831.84	2766.26	13.57	R207	1264.74	1256.22	10.47
C108	2828.69	2743.48	12.91	R208	1226.37	1197.64	10.82
C109	2722.68	2680.25	10.78	R209	1347.05	1340.94	15.91
C201	2219.36	2172.00	21.67	R210	1324.15	1317.29	17.31
C202	2181.98	2146.84	27.20	R211	1249.87	1234.88	10.25
C203	2200.48	2164.29	18.55	RC101	2706.54	2692.87	15.27
C204	1986.42	1965.23	20.71	RC102	2510.28	2491.92	14.52
C205	2187.12	2146.43	25.25	RC103	2241.36	2225.65	12.18
C206	2191.19	2131.93	22.49	RC104	2113.59	2096.31	11.66
C207	2209.41	2144.89	20.55	RC105	2444.51	2411.61	12.53
C208	1953.13	1939.74	21.62	RC106	2313.97	2297.32	12.80
R101	2503.41	2474.84	15.02	RC107	2149.40	2137.05	12.07
R102	2243.48	2203.63	14.44	RC108	2098.20	2085.27	11.03
R103	2064.96	2010.20	14.21	RC201	1910.04	1899.99	10.48
R104	1859.18	1823.57	11.79	RC202	1827.69	1805.97	10.34
R105	2172.92	2144.85	15.19	RC203	1650.80	1635.48	10.78
R106	2077.54	2050.30	13.61	RC204	1540.14	1528.16	15.05
R107	1896.07	1885.73	13.14	RC205	1775.22	1762.93	14.36
R108	1837.45	1821.86	13.04	RC206	1761.74	1758.77	12.06
R109	2009.20	1980.36	15.46	RC207	1615.10	1606.18	10.77
R110	1853.51	1817.21	12.37	RC208	1515.21	1501.71	10.71
R111	1870.58	1845.14	12.65				
R112	1811.04	1794.09	12.25				

Table B6: Detailed results for the large-scale HEVRP-NL instances of Group C (100 customers and 21 CSs)

Instance	Avg 10	BKS	Time (min)	Instance	Avg 10	Best 10	Time (min)
C101	2130.07	2122.79	11.71	R201	1419.85	1408.99	22.50
C102	2053.76	2042.43	11.16	R202	1251.24	1242.21	17.27
C103	2030.14	2025.88	10.71	R203	1127.75	1112.64	15.60
C104	1872.26	1861.43	9.80	R204	984.07	977.72	10.43
C105	2100.78	2082.03	11.47	R205	1222.34	1213.20	18.32
C106	2088.40	2077.03	12.26	R206	1165.35	1148.24	17.23
C107	2079.10	2069.54	12.03	R207	1053.21	1031.22	10.33
C108	2067.39	2053.48	11.59	R208	987.20	972.67	10.89
C109	1998.03	1982.39	11.00	R209	1132.23	1125.83	16.42
C201	1614.64	1594.90	23.98	R210	1119.55	1083.10	15.17
C202	1764.10	1748.93	17.75	R211	1028.30	1001.74	10.03
C203	1538.58	1522.12	22.45	RC101	2296.80	2289.97	14.85
C204	1475.09	1446.88	24.10	RC102	2089.81	2078.69	13.46
C205	1576.58	1550.86	22.33	RC103	1861.40	1853.01	11.03
C206	1465.44	1451.94	26.72	RC104	1716.97	1703.78	11.30
C207	1451.59	1443.92	26.04	RC105	2029.13	2018.77	12.31
C208	1447.63	1439.74	21.59	RC106	1947.77	1920.73	12.91
R101	2175.69	2154.77	15.19	RC107	1770.20	1757.14	12.17
R102	1916.49	1899.94	13.96	RC108	1712.16	1696.97	12.06
R103	1712.27	1694.55	15.25	RC201	1615.78	1589.99	10.04
R104	1518.11	1509.26	11.83	RC202	1494.37	1481.90	10.29
R105	1850.94	1837.85	14.79	RC203	1325.15	1310.48	10.69
R106	1751.07	1744.79	13.79	RC204	1202.57	1190.72	15.54
R107	1586.44	1575.83	12.74	RC205	1468.89	1440.36	14.85
R108	1478.55	1465.58	11.05	RC206	1445.14	1431.41	10.72
R109	1647.12	1634.29	12.52	RC207	1291.75	1273.23	10.95
R110	1519.37	1505.30	11.39	RC208	1183.73	1171.71	10.79
R111	1524.64	1511.15	14.83				
R112	1473.96	1453.34	12.23				

Table C1: Detailed comparison results for the E-VRP-NL benchmark (instances with 10, 20, or 40 customers)

Instance	ILS+HC			LNS			ILS			ILS+SP			
	Best	Avg	T	Best	Avg	T	Best	Avg	T	Best	Avg	T	Best Gap
tc0c10s2cf1	19.75	20.12	4	19.75	19.77	8	19.75	19.75	5	**19.75**	19.75	5	0.00%
tc0c10s2ct1	12.30	12.34	4	12.30	12.31	8	12.30	12.30	3	**12.30**	12.30	4	0.00%
tc0c10s3cf1	19.75	20.12	4	19.75	19.76	7	19.75	19.75	5	**19.75**	19.75	4	0.00%
tc0c10s3ct1	10.80	10.80	5	10.80	10.81	8	10.80	10.80	5	**10.80**	10.80	3	0.00%
tc1c10s2cf2	9.03	9.07	2	9.03	9.04	9	9.03	9.03	4	**9.03**	9.03	3	0.00%
tc1c10s2cf3	16.37	16.37	6	16.37	16.38	9	16.37	16.37	5	**16.37**	16.37	5	0.00%
tc1c10s2cf4	16.10	16.10	5	16.10	16.11	7	16.10	16.10	5	**16.10**	16.10	4	0.00%
tc1c10s2ct2	10.75	10.75	4	10.75	10.76	8	10.75	10.75	3	**10.75**	10.75	4	0.00%
tc1c10s2ct3	13.17	13.18	8	13.17	13.18	9	13.17	13.17	6	**13.17**	13.17	4	0.00%
tc1c10s2ct4	13.83	13.83	5	13.83	13.84	9	13.83	13.83	5	**13.83**	13.83	4	0.00%
tc1c10s3cf2	9.03	9.06	2	9.03	9.04	10	9.03	9.03	5	**9.03**	9.03	3	0.00%
tc1c10s3cf3	16.37	16.37	6	16.37	16.39	8	16.37	16.37	3	**16.37**	16.37	5	0.00%
tc1c10s3cf4	14.90	14.90	7	14.90	14.91	8	14.90	14.90	2	**14.90**	14.90	5	0.00%
tc1c10s3ct2	9.20	9.34	5	9.20	9.21	9	9.20	9.20	6	**9.20**	9.20	3	0.00%
tc1c10s3ct3	13.02	13.02	10	13.02	13.03	7	13.02	13.02	5	**13.02**	13.02	4	0.00%
tc1c10s3ct4	13.21	13.21	6	13.21	13.22	9	13.21	13.21	5	**13.21**	13.21	4	0.00%
tc2c10s2cf0	21.77	21.77	9	21.77	21.78	8	21.77	21.77	6	**21.77**	21.77	4	0.00%
tc2c10s2ct0	12.45	12.45	5	12.45	12.46	8	12.45	12.45	6	**12.45**	12.45	3	0.00%
tc2c10s3cf0	21.77	21.77	9	21.77	21.79	7	21.77	21.77	3	**21.77**	21.77	4	0.00%
tc2c10s3ct0	11.51	11.54	7	11.51	11.52	9	11.51	11.51	5	**11.51**	11.51	3	0.00%
tc0c20s3cf2	27.60	27.66	12	27.47	27.52	12	27.47	27.47	10	**27.47**	27.47	7	0.00%
tc0c20s3ct2	17.08	17.13	8	17.08	17.11	18	17.08	17.08	6	**17.08**	17.08	6	0.00%
tc0c20s4cf2	27.48	27.61	13	27.60	27.65	14	27.47	27.47	9	**27.47**	27.47	7	0.00%
tc0c20s4ct2	16.99	17.10	9	16.99	17.02	16	16.99	16.99	9	**16.99**	16.99	6	0.00%
tc1c20s3cf1	17.50	17.53	12	17.50	17.53	13	17.49	17.49	10	**17.49**	17.49	6	0.00%
tc1c20s3cf3	16.63	16.78	8	16.48	16.50	17	16.44	16.44	7	**16.44**	16.44	8	0.00%
tc1c20s3cf4	17.00	17.00	4	17.00	17.03	15	17.00	17.00	5	**17.00**	17.00	7	0.00%
tc1c20s3ct1	18.95	19.38	15	18.95	18.97	14	18.94	18.94	9	**18.94**	18.94	8	0.00%
tc1c20s3ct3	12.65	12.72	9	12.60	12.62	17	12.60	12.60	9	**12.60**	12.60	7	0.00%
tc1c20s3ct4	16.21	16.25	5	16.21	16.24	11	16.21	16.21	8	**16.21**	16.21	8	0.00%
tc1c20s4cf1	16.39	16.40	13	16.47	16.49	18	16.38	16.38	6	**16.38**	16.38	9	0.00%
tc1c20s4cf3	16.56	16.80	9	16.48	16.51	11	16.44	16.44	11	**16.44**	16.44	8	0.00%
tc1c20s4cf4	17.00	17.00	4	17.00	17.03	15	17.00	17.00	8	**17.00**	17.00	7	0.00%
tc1c20s4ct1	18.25	18.32	16	18.25	18.28	18	17.80	17.80	11	**17.80**	17.80	6	0.00%
tc1c20s4ct3	14.43	14.50	8	14.43	14.46	12	14.43	14.43	7	**14.43**	14.43	8	0.00%
tc1c20s4ct4	17.00	17.00	6	17.00	17.03	11	17.00	17.00	6	**17.00**	17.00	8	0.00%
tc2c20s3cf0	24.68	24.68	14	24.68	24.70	11	24.68	24.68	7	**24.68**	24.68	8	0.00%
tc2c20s3ct0	25.79	25.79	15	25.79	25.83	15	25.79	25.79	10	**25.79**	25.79	10	0.00%
tc2c20s4cf0	24.67	24.69	15	24.67	24.71	13	24.67	24.67	11	**24.67**	24.67	9	0.00%
tc2c20s4ct0	26.02	26.02	15	26.03	26.07	16	26.02	26.02	9	**26.02**	26.02	8	0.00%
tc0c40s5cf0	32.67	33.25	24	32.67	32.75	52	32.20	32.30	16	**32.20**	32.20	17	0.00%
tc0c40s5cf4	30.77	31.49	33	30.60	30.69	49	30.25	30.25	22	**30.25**	30.25	20	0.00%
tc0c40s5ct0	28.72	29.35	25	28.70	28.78	46	27.91	27.91	17	**27.91**	27.91	20	0.00%
tc0c40s5ct4	28.63	28.72	33	29.17	29.25	59	28.63	28.63	18	**28.63**	28.63	29	0.00%
tc0c40s8cf0	31.28	32.02	34	31.23	31.31	63	30.40	30.40	18	**30.40**	30.40	24	0.00%
tc0c40s8cf4	29.32	29.86	43	28.25	28.30	52	28.11	28.23	25	**28.11**	28.11	26	0.00%
tc0c40s8ct0	26.35	26.89	29	26.22	26.27	58	26.22	26.22	17	**26.22**	26.22	22	0.00%
tc0c40s8ct4	29.20	29.27	47	29.22	29.28	48	29.07	29.07	22	**29.07**	29.07	24	0.00%
tc1c40s5cf1	65.16	66.03	44	65.52	65.67	33	64.51	64.51	25	**64.51**	64.78	26	0.00%
tc1c40s5ct1	52.68	53.36	59	52.60	52.72	40	52.33	52.33	23	**52.33**	52.33	19	0.00%
tc1c40s8cf1	40.75	42.33	70	41.63	41.71	34	40.64	40.64	21	**40.64**	40.64	18	0.00%
tc1c40s8ct1	40.56	41.19	71	40.56	40.67	49	40.18	40.18	24	**40.18**	40.18	19	0.00%
tc2c40s5cf2	27.54	27.67	32	27.54	27.62	42	27.54	27.54	17	**27.54**	27.54	14	0.00%
tc2c40s5cf3	19.74	20.18	17	19.65	19.70	50	19.65	19.65	21	**19.65**	19.65	12	0.00%
tc2c40s5ct2	26.91	27.02	23	26.91	26.99	42	26.91	26.91	14	**26.91**	26.91	15	0.00%
tc2c40s5ct3	23.54	23.77	26	23.71	23.75	51	23.39	23.39	22	**23.39**	23.39	22	0.00%
tc2c40s8cf2	27.15	27.31	29	27.14	27.20	35	27.13	27.13	16	**27.13**	27.13	15	0.00%
tc2c40s8cf3	19.66	20.24	19	19.65	19.69	36	19.65	19.65	22	**19.65**	19.65	17	0.00%
tc2c40s8ct2	26.33	26.71	26	26.29	26.34	40	26.28	26.28	16	**26.28**	26.28	16	0.00%
tc2c40s8ct3	22.71	23.23	25	22.45	22.52	30	22.45	22.45	24	**22.45**	22.45	20	0.00%

ILS+HC: Montoya et al. (2017), LNS: Koç et al. (2019), ILS: Froger et al. (2022).

Table C2: Detailed comparison results for the E-VRP-NL benchmark (instances with 80, 160, or 320 customers)

Instance	ILS+HC			LNS			ILS			ILS+SP			
	Best	Avg	T	Best	Avg	T	Best	Avg	T	Best	Avg	T	Best Gap
tc0c80s12cf0	34.64	35.59	57	35.24	35.40	105	34.16	34.16	66	**34.06**	34.34	80	-0.29%
tc0c80s12cf1	42.90	44.07	75	42.30	42.47	85	40.91	40.94	68	**40.48**	40.69	87	-1.05%
tc0c80s12ct0	39.31	39.83	66	39.27	39.41	86	**37.51**	38.08	65	37.57	38.21	76	0.16%
tc0c80s12ct1	41.94	43.03	73	41.64	41.83	103	39.91	40.06	59	**39.72**	39.75	72	-0.48%
tc0c80s8cf0	39.43	39.86	56	40.64	40.77	88	39.08	39.16	48	**38.59**	39.09	53	-1.25%
tc0c80s8cf1	45.23	45.73	121	46.65	46.80	98	43.38	43.95	73	**43.38**	43.78	85	0.00%
tc0c80s8ct0	41.90	42.76	54	41.44	41.59	87	40.52	41.44	61	**40.52**	41.36	54	0.00%
tc0c80s8ct1	45.27	45.85	130	45.25	45.37	100	43.85	44.07	73	**43.85**	43.85	83	0.00%
tc1c80s12cf2	29.54	30.73	61	29.54	29.66	113	28.65	28.77	52	**28.58**	28.68	72	-0.24%
tc1c80s12ct2	29.52	30.66	59	29.38	29.47	114	28.73	29.18	54	**28.66**	28.88	79	-0.24%
tc1c80s8cf2	30.81	31.83	51	31.38	31.47	94	29.15	29.15	51	**29.03**	29.16	78	-0.41%
tc1c80s8ct2	31.74	32.36	60	31.72	31.82	98	30.45	30.52	57	**30.11**	30.21	76	-1.12%
tc2c80s12cf3	31.97	32.70	76	31.28	31.37	105	30.60	30.60	57	**30.60**	30.60	68	0.00%
tc2c80s12cf4	43.89	44.97	131	43.69	43.81	86	42.10	42.14	83	**42.10**	42.13	111	0.00%
tc2c80s12ct3	30.83	31.59	58	30.31	30.39	114	29.90	29.90	54	**29.90**	29.91	71	0.00%
tc2c80s12ct4	42.40	42.82	134	42.56	44.68	103	40.27	40.27	74	**40.27**	40.75	90	0.00%
tc2c80s8cf3	32.44	32.60	64	31.94	32.06	87	31.70	31.93	55	**31.60**	31.95	66	-0.32%
tc2c80s8cf4	49.29	49.69	100	49.67	49.84	128	46.03	46.78	93	**45.36**	46.07	98	-1.46%
tc2c80s8ct3	32.31	32.55	65	32.71	32.82	89	31.38	31.43	65	**31.38**	31.68	76	0.00%
tc2c80s8ct4	44.83	46.61	111	44.16	44.31	103	43.83	44.00	75	**43.72**	43.92	83	-0.25%
tc0c160s16cf2	61.20	62.99	365	62.09	62.55	442	57.91	58.00	242	**57.91**	57.98	326	0.00%
tc0c160s16cf4	82.92	83.84	1213	82.77	83.41	709	76.90	77.55	367	**76.83**	77.29	450	-0.09%
tc0c160s16ct2	59.90	62.80	342	59.75	60.29	811	57.64	57.73	247	**57.64**	58.02	311	0.00%
tc0c160s16ct4	82.37	83.08	945	82.90	83.85	983	76.14	76.90	353	**75.60**	76.29	428	-0.71%
tc0c160s24cf2	59.27	60.92	403	59.26	59.79	732	56.32	56.76	253	**56.12**	56.55	341	-0.36%
tc0c160s24cf4	81.44	82.13	1209	81.43	82.33	595	**75.53**	76.30	370	75.63	76.60	494	0.13%
tc0c160s24ct2	59.25	60.19	410	59.67	60.21	915	**55.42**	56.47	253	55.61	56.64	305	0.34%
tc0c160s24ct4	80.96	82.11	957	81.38	82.21	436	**75.05**	75.87	372	75.25	76.22	468	0.27%
tc1c160s16cf0	79.80	80.75	766	79.76	80.52	420	74.54	75.32	327	**74.54**	75.39	395	0.00%
tc1c160s16cf3	71.76	72.75	462	71.98	72.77	729	**66.45**	67.20	307	66.72	67.17	312	0.41%
tc1c160s16ct0	79.04	79.90	643	80.21	80.99	472	74.20	75.31	326	**74.20**	75.14	470	0.00%
tc1c160s16ct3	73.29	75.11	279	73.24	73.82	750	65.31	66.20	289	**65.30**	65.67	384	-0.02%
tc1c160s24cf0	78.60	79.30	741	79.48	80.32	460	73.62	74.05	331	**73.62**	74.19	356	0.00%
tc1c160s24cf3	68.56	69.57	483	68.73	69.28	522	**62.90**	63.64	282	63.17	63.22	329	0.43%
tc1c160s24ct0	78.21	79.35	578	78.32	79.05	553	73.34	74.00	319	**73.33**	73.88	523	-0.01%
tc1c160s24ct3	68.72	69.98	358	69.17	69.76	889	63.19	63.66	280	**62.86**	63.36	384	-0.52%
tc2c160s16cf1	60.34	61.26	274	60.25	60.70	716	56.65	57.39	252	**56.00**	56.62	327	-1.15%
tc2c160s16ct1	60.27	60.62	288	59.86	60.40	408	55.37	55.52	232	**55.37**	55.54	321	0.00%
tc2c160s24cf1	59.82	61.14	305	60.01	60.63	564	**56.70**	57.27	260	57.16	58.05	386	0.81%
tc2c160s24ct1	59.13	59.72	340	59.97	60.53	531	55.03	55.15	238	**55.03**	55.41	351	0.00%
tc1c320s24cf2	152.13	153.99	7106	153.12	154.65	4155	133.32	133.99	1287	**132.39**	133.72	1667	-0.70%
tc1c320s24cf3	117.48	118.36	3066	117.39	118.43	3258	106.43	107.00	1060	**105.98**	106.69	1492	-0.42%
tc1c320s24ct2	148.77	154.13	6853	148.57	149.89	4727	131.63	132.49	1231	**131.25**	131.39	1206	-0.29%
tc1c320s24ct3	116.64	119.17	3274	117.50	118.53	5105	**105.93**	106.67	1045	105.99	106.82	1376	0.06%
tc1c320s38cf2	141.63	147.08	7236	142.25	144.17	4249	129.19	129.76	1178	**129.02**	129.74	1435	-0.13%
tc1c320s38cf3	116.22	117.74	3114	117.31	118.78	5978	106.01	106.36	1129	**106.00**	106.71	1405	-0.01%
tc1c320s38ct2	140.96	145.09	6974	142.75	144.50	6078	128.82	129.51	1167	**128.45**	128.47	1037	-0.29%
tc1c320s38ct3	116.07	117.71	3063	117.91	119.40	3157	105.73	106.74	1186	**105.29**	106.26	1566	-0.42%
tc2c320s24cf0	182.45	186.94	6566	182.90	185.27	4014	**158.80**	160.55	1343	159.32	161.16	1882	0.33%
tc2c320s24cf1	95.51	96.42	1456	95.71	96.81	5150	87.46	87.64	890	**87.32**	87.71	1197	-0.16%
tc2c320s24cf4	122.74	124.68	3681	122.83	124.51	3923	**111.16**	111.62	989	111.98	112.06	1210	0.74%
tc2c320s24ct0	181.45	186.23	7204	182.29	183.80	6191	159.70	160.49	1309	**159.70**	162.20	1927	0.00%
tc2c320s24ct1	94.73	96.49	1259	94.97	95.96	3530	**87.25**	87.83	863	87.51	88.12	1037	0.30%
tc2c320s24ct4	121.94	123.85	4274	122.09	123.45	5196	111.09	111.62	1041	**111.07**	111.43	1569	-0.02%
tc2c320s38cf0	176.92	182.31	6734	178.17	179.81	3350	**158.70**	159.53	1356	159.25	160.41	1951	0.35%
tc2c320s38cf1	94.29	95.07	1602	95.73	96.79	5343	86.92	87.25	890	**86.91**	87.37	1145	-0.01%
tc2c320s38cf4	122.32	123.47	2661	122.26	123.46	3724	109.80	110.66	1087	**109.54**	110.56	1838	-0.24%
tc2c320s38ct0	190.97	192.15	7637	192.23	194.66	4448	158.71	159.35	1374	**157.89**	159.45	2075	-0.52%
tc2c320s38ct1	94.53	95.29	1409	94.66	95.87	3973	86.59	86.97	894	**86.34**	86.53	1061	-0.29%
tc2c320s38ct4	121.66	123.15	2785	121.64	123.06	5554	110.05	110.55	1034	**109.55**	109.61	1375	-0.45%

ILS+HC: Montoya et al. (2017), LNS: Koç et al. (2019), ILS: Froger et al. (2022).

Table D1: Comparision results of the BKS for the E-FSMFTW-PR instances (100 customers and 21 charging stations)

Instance	Group A			Group B			Group C		
	LNS+SP	ILS+SP		LNS+SP	ILS+SP		LNS+SP	ILS+SP	
	Best	Best 10	Time	Best	Best 10	Time	Best	Best 10	Time
C101	7158.74	**7158.74**	17.11	2481.50	**2481.50**	7.52	1791.50	**1791.50**	8.38
C102	7134.84	**7134.84**	18.02	2433.02	**2433.02**	7.78	1743.02	**1743.02**	8.15
C103	7113.05	**7113.05**	25.90	2412.04	**2412.04**	8.27	1735.62	**1735.62**	8.15
C104	7096.91	**7096.91**	36.35	2352.38	**2352.22**	8.39	1646.69	**1646.69**	7.15
C105	7138.85	**7138.27**	20.96	2452.22	**2452.22**	8.83	1760.56	**1760.56**	8.93
C106	7134.75	**7134.75**	26.20	2448.31	**2448.31**	9.21	1756.07	**1756.07**	8.31
C107	7137.57	**7136.44**	16.73	2446.00	**2446.00**	8.03	1756.00	**1756.00**	7.95
C108	7130.50	**7130.50**	17.37	2439.37	**2435.32**	8.29	1747.58	**1747.58**	8.21
C109	7113.94	**7113.94**	11.31	2388.13	**2383.51**	7.29	1688.99	**1688.99**	8.12
C201	5690.68	**5690.68**	12.67	1690.68	**1690.68**	11.88	1190.68	**1190.68**	11.79
C202	5690.68	**5690.68**	12.85	1690.68	**1690.68**	11.84	1190.68	**1190.68**	11.79
C203	5689.56	**5689.56**	13.45	1689.56	**1689.56**	11.50	1183.42	**1183.42**	12.95
C204	5688.58	**5688.58**	12.44	1688.58	**1688.58**	11.96	1174.05	**1174.05**	10.55
C205	5687.96	**5687.96**	12.10	1687.96	**1687.96**	12.03	1183.42	**1183.42**	13.11
C206	5687.96	**5687.96**	12.81	1687.96	**1687.96**	12.42	1183.42	**1183.42**	12.06
C207	5687.96	**5687.96**	12.88	1687.96	**1687.96**	12.86	1183.42	**1183.42**	12.09
C208	5681.47	**5681.47**	11.40	1681.47	**1681.47**	11.72	1181.47	**1181.47**	10.42
R101	4337.03	**4333.42**	9.71	2208.83	**2204.22**	9.47	1918.46	**1918.46**	12.24
R102	4175.17	**4166.26**	10.50	2030.15	**2022.36**	8.23	1737.57	**1735.16**	9.08
R103	4038.30	**4038.30**	9.95	1868.31	**1868.31**	8.64	1541.75	**1541.39**	9.59
R104	3966.74	**3966.74**	9.02	1739.69	**1732.11**	8.07	1410.83	1414.09	7.75
R105	4138.01	**4138.01**	10.52	1987.72	**1987.72**	10.21	1666.55	**1666.55**	10.30
R106	4063.48	**4063.48**	8.92	1915.27	**1908.35**	9.11	1590.78	**1590.34**	9.31
R107	4013.59	**4013.59**	9.55	1791.63	**1791.63**	9.04	1462.24	**1458.32**	8.65
R108	3963.85	**3963.85**	8.73	1715.41	**1698.13**	7.77	1381.43	**1371.12**	7.90
R109	4024.32	**4024.32**	9.43	1846.35	1848.60	9.11	1523.63	**1523.63**	9.27
R110	3975.70	**3975.70**	8.75	1740.14	**1740.14**	7.86	1412.69	**1412.69**	8.71
R111	3980.31	**3980.31**	9.58	1762.41	**1738.10**	7.88	1425.06	**1425.06**	8.52
R112	3953.02	**3953.02**	8.51	1703.83	**1694.63**	7.93	1381.48	**1368.18**	8.02
R201	3395.95	**3395.95**	11.93	1585.94	**1585.06**	13.61	1362.76	**1362.76**	12.26
R202	3262.42	**3262.42**	10.21	1461.58	1465.39	10.85	1236.59	**1236.59**	9.15
R203	3129.85	**3129.85**	10.17	1328.73	**1328.41**	11.22	1103.41	**1103.41**	10.41
R204	3007.93	**3007.93**	7.63	1207.03	**1207.03**	8.29	977.72	**977.72**	7.23
R205	3233.90	**3233.90**	11.82	1436.10	**1436.10**	11.65	1197.20	**1197.20**	10.44
R206	3156.58	**3156.58**	11.14	1356.87	**1356.87**	10.76	1131.92	**1131.92**	9.19
R207	3063.74	**3063.74**	8.06	1256.22	**1256.22**	7.72	1031.22	**1031.22**	7.37
R208	2997.62	**2997.62**	8.28	1195.96	**1195.96**	7.54	971.46	**971.46**	7.94
R209	3131.89	**3131.13**	10.27	1322.11	**1322.11**	10.64	1092.06	**1092.06**	9.60
R210	3108.36	**3108.36**	11.25	1308.13	**1308.13**	9.70	1074.83	**1074.83**	9.65
R211	3032.10	**3032.10**	7.40	1234.88	**1234.88**	8.23	1001.74	**1001.74**	6.68
RC101	5226.08	**5226.08**	9.28	2459.71	**2455.43**	10.54	2051.62	**2051.62**	10.46
RC102	5060.23	**5057.16**	9.46	2265.88	**2265.88**	8.95	1881.00	**1881.00**	9.48
RC103	4901.78	**4901.78**	9.09	2099.69	**2085.24**	8.77	1723.03	**1709.10**	8.10
RC104	4755.07	**4755.07**	9.74	1970.95	**1942.66**	7.91	1562.87	**1560.56**	7.44
RC105	5047.25	**5047.25**	9.34	2204.38	**2204.38**	7.76	1835.54	**1835.54**	8.16
RC106	4988.19	**4988.19**	9.25	2186.23	**2156.34**	8.91	1770.28	**1770.28**	9.51
RC107	4826.45	**4802.43**	8.38	1994.17	**1990.76**	8.83	1619.17	**1619.17**	8.20
RC108	4788.68	**4786.90**	9.10	1925.85	**1925.85**	8.42	1565.27	**1565.27**	8.57
RC201	4337.60	**4337.60**	6.92	1899.99	**1899.99**	6.52	1588.25	**1588.25**	6.80
RC202	4261.89	**4261.89**	5.71	1805.24	**1805.24**	7.19	1481.05	**1481.05**	7.59
RC203	4147.68	**4147.68**	6.57	1635.48	**1635.48**	8.61	1310.37	**1310.37**	7.13
RC204	4106.90	**4106.90**	7.69	1520.59	**1520.59**	9.75	1182.32	**1182.32**	9.84
RC205	4254.70	**4243.62**	6.78	1749.64	**1749.64**	10.09	1410.99	**1410.99**	8.26
RC206	4244.04	**4244.04**	6.39	1750.32	1754.00	8.14	1430.32	**1430.32**	7.60
RC207	4172.61	**4172.61**	6.69	1606.18	**1606.18**	8.59	1273.23	**1273.23**	7.76
RC208	4103.44	**4103.44**	7.57	1495.34	**1495.34**	9.44	1165.34	1167.19	7.94
Avg	4750.65	**4749.67**	11.43	1838.05	**1835.22**	9.32	1438.94	**1438.19**	9.11

LNS+SP: Wang & Zhao (2023)